Designation: E1441 – 11

Standard Guide for Computed Tomography (CT) Imaging[1]

This standard is issued under the fixed designation E1441; the number immediately following the designation indicates the year of original adoption or, in the case of revision, the year of last revision. A number in parentheses indicates the year of last reapproval. A superscript epsilon (ε) indicates an editorial change since the last revision or reapproval.

This standard has been approved for use by agencies of the U.S. Department of Defense.

1. Scope*

1.1 Computed tomography (CT) is a radiographic method that provides an ideal examination technique whenever the primary goal is to locate and size planar and volumetric detail in three dimensions. Because of the relatively good penetrability of X-rays, as well as the sensitivity of absorption cross sections to atomic chemistry, CT permits the nondestructive physical and, to a limited extent, chemical characterization of the internal structure of materials. Also, since the method is X-ray based, it applies equally well to metallic and nonmetallic specimens, solid and fibrous materials, and smooth and irregularly surfaced objects. When used in conjunction with other nondestructive evaluation (NDE) methods, such as ultrasound, CT data can provide evaluations of material integrity that cannot currently be provided nondestructively by any other means.

1.2 This guide is intended to satisfy two general needs for users of industrial CT equipment: (*1*) the need for a tutorial guide addressing the general principles of X-ray CT as they apply to industrial imaging; and (*2*) the need for a consistent set of CT performance parameter definitions, including how these performance parameters relate to CT system specifications. Potential users and buyers, as well as experienced CT inspectors, will find this guide a useful source of information for determining the suitability of CT for particular examination problems, for predicting CT system performance in new situations, and for developing and prescribing new scan procedures.

1.3 This guide does not specify test objects and test procedures for comparing the relative performance of different CT systems; nor does it treat CT inspection techniques, such as the best selection of scan parameters, the preferred implementation of scan procedures, the analysis of image data to extract densitometric information, or the establishment of accept/reject criteria for a new object.

1.4 Standard practices and methods are not within the purview of this guide. The reader is advised, however, that examination practices are generally part and application specific, and industrial CT usage is new enough that in many instances a consensus has not yet emerged. The situation is complicated further by the fact that CT system hardware and performance capabilities are still undergoing significant evolution and improvement. Consequently, an attempt to address generic examination procedures is eschewed in favor of providing a thorough treatment of the principles by which examination methods can be developed or existing ones revised.

1.5 The principal advantage of CT is that it nondestructively provides quantitative densitometric (that is, density and geometry) images of thin cross sections through an object. Because of the absence of structural noise from detail outside the thin plane of inspection, images are much easier to interpret than conventional radiographic data. The new user can learn quickly (often upon first exposure to the technology) to read CT data because the images correspond more closely to the way the human mind visualizes three-dimensional structures than conventional projection radiography. Further, because CT images are digital, they may be enhanced, analyzed, compressed, archived, input as data into performance calculations, compared with digital data from other NDE modalities, or transmitted to other locations for remote viewing. Additionally, CT images exhibit enhanced contrast discrimination over compact areas larger than 20 to 25 pixels. This capability has no classical analog. Contrast discrimination of better than 0.1 % at three-sigma confidence levels over areas as small as one-fifth of one percent the size of the object of interest are common.

1.6 With proper calibration, dimensional inspections and absolute density determinations can also be made very accurately. Dimensionally, virtually all CT systems provide a pixel resolution of roughly 1 part in 1000 , and metrological algorithms can often measure dimensions to one-tenth of one pixel or so with three-sigma accuracies. For small objects (less than 100 mm (4 in.) in diameter), this translates into accuracies of approximately 0.1 mm (0.003 to 0.005 in.) at three-sigma. For much larger objects, the corresponding figure will be proportionally greater. Attenuation values can also be related accurately to material densities. If details in the image are

[1] This guide is under the jurisdiction of ASTM Committee E07 on Nondestructive Testing and is the direct responsibility of Subcommittee E07.01 on Radiology (X and Gamma) Method.

Current edition approved July 1, 2011. Published July 2011. Originally approved in 1991. Last previous edition approved in 2005 as E1441 - 00(2005). DOI: 10.1520/E1441-11.

***A Summary of Changes section appears at the end of this standard**

known to be pure homogeneous elements, the density values may still be sufficient to identify materials in some cases. For the case in which no *a priori* information is available, CT densities cannot be used to identify unknown materials unambiguously, since an infinite spectrum of compounds can be envisioned that will yield any given observed attenuation. In this instance, the exceptional density sensitivity of CT can still be used to determine part morphology and highlight structural irregularities.

1.7 In some cases, dual energy (DE) CT scans can help identify unknown components. DE scans provide accurate electron density and atomic number images, providing better characterizations of the materials. In the case of known materials, the additional information can be traded for improved conspicuity, faster scans, or improved characterization. In the case of unknown materials, the additional information often allows educated guesses on the probable composition of an object to be made.

1.8 As with any modality, CT has its limitations. The most fundamental is that candidate objects for examination must be small enough to be accommodated by the handling system of the CT equipment available to the user and radiometrically translucent at the X-ray energies employed by that particular system. Further, CT reconstruction algorithms require that a full 180 degrees of data be collected by the scanner. Object size or opacity limits the amount of data that can be taken in some instances. While there are methods to compensate for incomplete data which produce diagnostically useful images, the resultant images are necessarily inferior to images from complete data sets. For this reason, complete data sets and radiometric transparency should be thought of as requirements. Current CT technology can accommodate attenuation ranges (peak-to-lowest-signal ratio) of approximately four orders of magnitude. This information, in conjunction with an estimate of the worst-case chord through a new object and a knowledge of the average energy of the X-ray flux, can be used to make an educated guess on the feasibility of scanning a part that has not been examined previously.

1.9 Another potential drawback with CT imaging is the possibility of artifacts in the data. As used here, an artifact is anything in the image that does not accurately reflect true structure in the part being inspected. Because they are not real, artifacts limit the user's ability to quantitatively extract density, dimensional, or other data from an image. Therefore, as with any technique, the user must learn to recognize and be able to discount common artifacts subjectively. Some image artifacts can be reduced or eliminated with CT by improved engineering practice; others are inherent in the methodology. Examples of the former include scattered radiation and electronic noise. Examples of the latter include edge streaks and partial volume effects. Some artifacts are a little of both. A good example is the cupping artifact, which is due as much to radiation scatter (which can in principle be largely eliminated) as to the polychromaticity of the X-ray flux (which is inherent in the use of bremsstrahlung sources).

1.10 Depending on the technology of the CT system, complete three-dimensional CT examinations can be time consuming. Thus, less than 100 % CT examinations are often necessary or must be accommodated by complementing the inspection process with digital radiographic screening. One partial response to this problem is to use large slice thicknesses. This leads to reduced axial resolution and can introduce partial volume artifacts in some cases; however, this is an acceptable tradeoff in many instances. In principle, this drawback can be eliminated by resorting to full volumetric scans using planar detectors instead of linear detectors (see (*1*) under 6.5.1.5).

1.11 Complete part examinations demand large storage capabilities or advanced display techniques, or both, and equipment to help the operator review the huge volume of data generated. This can be compensated for by state-of-the-art graphics hardware and automatic examination software to aid the user. However, automated accept/reject software is object dependent and to date has been developed and employed in only a limited number of cases.

1.12 *Units*—The values stated in SI units are to be regarded as standard. The values given in parentheses are mathematical conversions to inch-pound units that are provided for information only and are not considered standard.

1.13 *This standard does not purport to address all of the safety concerns, if any, associated with its use. It is the responsibility of the user of this standard to establish appropriate safety and health practices and determine the applicability of regulatory limitations prior to use.*

2. Referenced Documents

2.1 *ASTM Standards:*[2]

E1316 Terminology for Nondestructive Examinations

E1570 Practice for Computed Tomographic (CT) Examination

3. Terminology

3.1 *Definitions*—CT, being a radiographic modality, uses much the same vocabulary as other X-ray techniques. A number of terms are not referenced, or are referenced without discussion, in Terminology E1316. Because they have meanings or carry implications unique to CT, they appear with explanation in Appendix X1. Throughout this guide, the term "X-ray" is used to denote penetrating electromagnetic radiation; however, electromagnetic radiation may be either X-rays or gamma rays.

3.2 *Acronyms:*

3.2.1 *BW*—beam width.

3.2.2 *CDD*—contrast-detail-dose.

3.2.3 *CT*—computed tomography.

3.2.4 *CAT*—computerized axial tomography.

3.2.5 *DR*—digital radiography.

3.2.6 *ERF*—edge response function.

3.2.7 *LSF*—line spread function.

[2] For referenced ASTM standards, visit the ASTM website, www.astm.org, or contact ASTM Customer Service at service@astm.org. For *Annual Book of ASTM Standards* volume information, refer to the standard's Document Summary page on the ASTM website.

3.2.8 *MTF*—modulation transfer function.

3.2.9 *NDE*—nondestructive evaluation.

3.2.10 *PDF*—probability distribution function.

3.2.11 *PSF*—point spread function.

4. Summary of Guide

4.1 This guide provides a tutorial introduction to the technology and terminology of CT. It deals extensively with the physical and mathematical basis of CT, discusses the basic hardware configuration of all CT systems, defines a comprehensive set of fundamental CT performance parameters, and presents a useful method of characterizing and predicting system performance. Also, extensive descriptions of terms and references to publications relevant to the subject are provided.

4.2 This guide is divided into three main sections. Sections 5 and 6 provide an overview of CT: defining the process, discussing the performance characteristics of CT systems, and describing the basic elements of all CT systems. Section 8 addresses the physical and mathematical basis of CT imaging. Section 8 addresses in more detail a number of important performance parameters as well as their characterization and verification. This section is more technical than the other sections, but it is probably the most important of all. It establishes a single, unified set of performance definitions and relates them to more basic system parameters with a few carefully selected mathematical formulae.

5. Significance and Use

5.1 This guide provides a tutorial introduction to the theory and use of computed tomography. This guide begins with a overview intended for the interested reader with a general technical background. Subsequent, more technical sections describe the physical and mathematical basis of CT technology, the hardware and software requirements of CT equipment, and the fundamental measures of CT performance. This guide includes an extensive glossary (with discussion) of CT terminology and an extensive list of references to more technical publications on the subject. Most importantly, this guide establishes consensus definitions for basic measures of CT performance, enabling purchasers and suppliers of CT systems and services to communicate unambiguously with reference to a recognized standard. This guide also provides a few carefully selected equations relating measures of CT performance to key system parameters.

5.2 *General Description of Computed Tomography*—CT is a radiographic inspection method that uses a computer to reconstruct an image of a cross-sectional plane (slice) through an object. The resulting cross-sectional image is a quantitative map of the linear X-ray attenuation coefficient, μ, at each point in the plane. The linear attenuation coefficient characterizes the local instantaneous rate at which X-rays are removed during the scan, by scatter or absorption, from the incident radiation as it propagates through the object (See 7.5). The attenuation of the X-rays as they interact with matter is a well-studied problem (**1**)[3] and is the result of several different interaction mechanisms. For industrial CT systems with peak X-ray energy below a few MeV, all but a few minor effects can be accounted for in terms of the sum of just two interactions: photoelectric absorption and Compton scattering (**1**). The photoelectric interaction is strongly dependent on the atomic number and density of the absorbing medium; the Compton scattering is predominantly a function of the electron density of the material. Photoelectric attenuation dominates at lower energies and becomes more important with higher atomic number, while Compton scattering dominates at higher energies and becomes more important at lower atomic number. In special situations, these dependencies can be used to advantage (see 7.6.2 and references therein).

5.2.1 One particularly important property of the total linear attenuation coefficient is that it is proportional to material density, which is of course a fundamental physical property of all matter. The fact that CT images are proportional to density is perhaps the principal virtue of the technology and the reason that image data are often thought of as representing the distribution of material density within the object being inspected. This is a dangerous oversimplification, however. The linear attenuation coefficient also carries an energy dependence that is a function of material composition. This feature of the attenuation coefficient may or may not (depending on the materials and the energies of the X-rays involved) be more important than the basic density dependence. In some instances, this effect can be detrimental, masking the density differences in a CT image; in other instances, it can be used to advantage, enhancing the contrast between different materials of similar density.

5.2.2 The fundamental difference between CT and conventional radiography is shown in Fig. 1. In conventional radiography, information on the slice plane "P" projects into a

[3] The boldface numbers in parentheses refer to the list of references at the end of this standard.

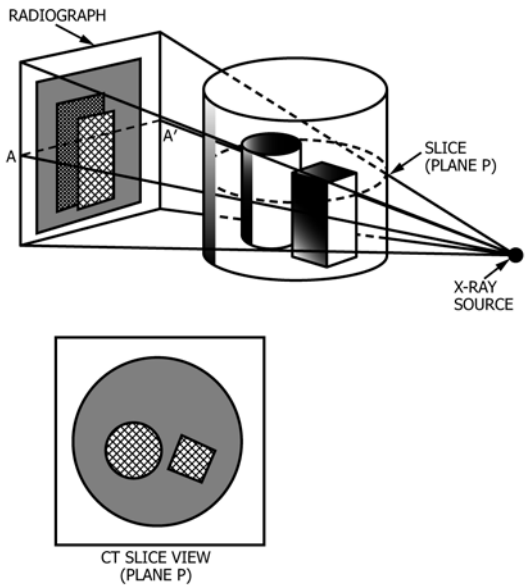

FIG. 1 A CT Image Versus a Conventional Radiograph

single line, "A-A;" whereas with the associated CT image, the full spatial information is preserved. CT information is derived from a large number of systematic observations at different viewing angles, and an image is then reconstructed with the aid of a computer. The image is generated in a series of discrete picture elements or pixels. A typical CT image might consist of a 512 by 512 or 1024 by 1024 array of attenuation values for a single cross-sectional slice through a test specimen. This resultant two-dimensional map of the slice plane is an image of the test article. Thus, by using CT, one can, in effect, slice open the test article, examine its internal features, record the different attenuations, perform dimensional inspections, and identify any material or structural anomalies that may exist. Further, by stacking and comparing adjacent CT slices of a test article, a three dimensional image of the interior can be constructed.

5.2.3 From Fig. 1, it can be appreciated readily that if an internal feature is detected in conventional projection radiography, its position along the line-of-sight between the source and the film is unknown. Somewhat better positional information can be determined by making additional radiographs from several viewing angles and triangulating. This triangulation is a rudimentary, manual form of tomographic reconstruction. In essence, a CT image is the result of triangulating every point in the plane from many different directions.

5.2.4 Because of the volume of data that must be collected and processed with CT, scans are usually made one slice at a time. A set of X-ray attenuation measurements is made along a set of paths projected at different locations around the periphery of the test article. The first part of Fig. 2 illustrates a set of measurements made on a test object containing two attenuating disks of different diameters. The X-ray attenuation measurement made at a particular angle, φ_1, is referred to as a single view. It is shown as $f_{\varphi 1}(x')$, where x' denotes the linear position of the measurement. The second part of Fig. 2 shows measurements taken at several other angles $f_{\varphi i}(x')$. Each of the attenuation measurements within these views is digitized and stored in a computer, where it is subsequently conditioned (for example, normalized and corrected) and filtered (convolved), as discussed in more detail in Section 7. The next step in image processing is to backproject the views, which is also shown in the second part of Fig. 2. Backprojection consists of projecting each view back along a line corresponding to the direction in which the projection data were collected. The backprojections, when enough views are employed, form a faithful reconstruction of the object. Even in this simple example, with only four projections, the concentration of backprojected rays already begins to show the relative size and position of features in the original object.

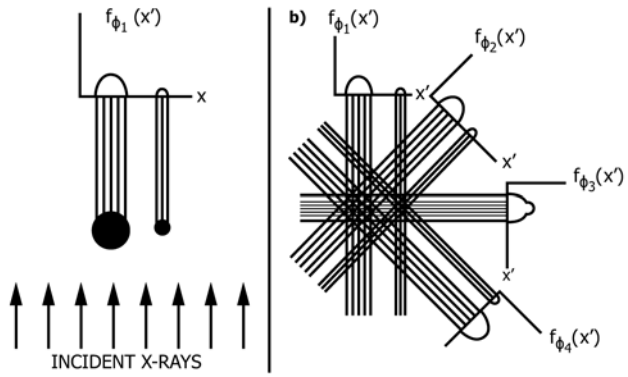

FIG. 2 Schematic Illustrations of How CT Works

5.3 *System Capabilities*—The ability of a CT system to image thin cross-sectional areas of interest through an object makes it a powerful complement to conventional radiographic inspections. Like any imaging system, a CT system can never duplicate exactly the object that is scanned. The extent to which a CT image does reproduce the object is dictated largely by the competing influences of the spatial resolution, the statistical noise, and the artifacts of the imaging system. Each of these aspects is discussed briefly here. A more complete discussion will be found in Sections 8 and 9.

5.3.1 *Spatial Resolution*—Radiographic imaging is possible because different materials have different X-ray attenuation coefficients. In CT, these X-ray coefficients are represented on a display monitor as shades of gray, similar to a photographic image, or in false color. The faithfulness of a CT image depends on a number of system-level performance factors, with one of the most important being spatial resolution. Spatial resolution refers to the ability of a CT system to resolve small details or locate small features with respect to some reference point.

5.3.1.1 Spatial resolution is generally quantified in terms of the smallest separation at which two points can be distinguished as separate entities. The limiting value of the spatial resolution is determined by the design and construction of the system and by the amount of data and sampling scheme used to interrogate the object of interest. The precision of the mechanical system determines how accurately the views can be backprojected, and the X-ray optics determine the fineness of the detail that can be resolved. The number of views and the number of single absorption measurements per view determine the size of the reconstruction matrix that can be faithfully reconstructed. Reducing pixel size can improve spatial resolution in an image until the inherent limit set by these constraints is reached. Beyond this limit, smaller pixels do not increase the spatial resolution and can induce artifacts in the image. However, under certain circumstances, reconstructing with pixels smaller than would otherwise be warranted can be a useful technique. For instance, when performing dimensional inspections, working from an image with pixels as small as one-fourth the sample spacing can provide measurable benefit.

5.3.1.2 It can also be shown that a given CT image is equivalent to the blurring (convolution) of the ideal representation of the object with a smooth, two-dimensional Gaussian-like function called the point-spread-function (PSF). The specification of the PSF of a system is an important characterization of a CT system and can be derived fairly accurately from the parameters of the CT system. The effect of the PSF is to blur the features in the CT image. This has two effects: (*1*) small objects appear larger and (*2*) sharp boundaries appear diffuse. Blurring the image of small objects reduces resolution since the images of two small point-like objects that are close together will overlap and may be indistinguishable from a

single feature. Blurring sharp edges reduces the perceptibility of boundaries of different materials for the same reason. This effect is especially important at interfaces between materials, where the possibility of separations of one type or another are of the greatest concern. Thus, knowledge of the PSF of a CT system is crucial to the quantitative specification of the maximum resolution and contrast achievable with that system.

5.3.1.3 It should be noted, since it is a common source of misunderstanding, that the smallest feature that can be detected in a CT image is not the same as the smallest that can be resolved. A feature considerably smaller than a single pixel can affect the pixel to which it corresponds to such an extent that it will appear with a visible contrast relative to adjacent pixels. This phenomenon, the "partial-volume effect," is discussed in 7.6. The difference between the resolution of a small feature and the resolution of its substructure is of fundamental importance for CT.

5.3.2 *Statistical Noise*—All images made from physical interactions of some kind will exhibit intrinsic statistical noise. In radiography, this noise arises from two sources: (*1*) intrinsic statistical variations due to the finite number of photons measured; and (*2*) the particular form of instrumentation and processing used. A good example in conventional radiography is film that has been underexposed. Even on a very uniform region of exposure, close examination of the film will reveal that only a small number of grains per unit area have been exposed. An example of instrumentation induced noise is the selection of coarse- or fine-grain film. If the films are exposed to produce an image with a given density, the fine-grain film will have lower statistical noise than the coarse-grain film. In CT, statistical noise in the image appears as a random variation superimposed on the CT level of the object. If a feature is small, it may be difficult to determine its median gray level and distinguish it from surrounding material. Thus, statistical noise limits contrast discrimination in a CT image.

5.3.2.1 Although statistical noise is unavoidable, its magnitude with respect to the desired signal can be reduced to some extent by attempting to increase the desired signal. This can be accomplished by increasing the scan time, the output of the X-ray source, or the size of the X-ray source and detectors. Increasing the detector and source size, however, will generally reduce spatial resolution. This tradeoff between spatial resolution and statistical noise is a fundamental characteristic of CT.

5.3.3 *Artifacts*—An artifact is something in an image that does not correspond to a physical feature in the test object. All imaging systems, whether CT or conventional radiography, exhibit artifacts. Examples of artifacts common to conventional radiography are blotches of underdevelopment on a film or scattering produced by high-density objects in the X-ray field. In both cases, familiarity with these artifacts allows the experienced radiographer to discount their presence qualitatively.

5.3.3.1 CT artifacts manifest themselves in somewhat different ways, since the CT image is calculated from a series of measurements. A common artifact is caused by beam hardening and manifests itself as cupping, that is, a false radial gradient in the density that causes abnormally low values at the interior center of a uniform object and high values at the periphery. Artifacts occurring at the interfaces between different density materials are more subtle. There is often an overshoot or undershoot in the density profile at such a density boundary. The interface density profile must be well characterized so that delaminations or separations are not obscured. If the interface profile is not well characterized, false positive indications of defects or, more importantly, situations in which defects go undetected will result. Thus it is important to understand the class of artifacts pertinent to the inspection and to put quantitative limits on particular types of artifacts. Some of the artifacts are inherent in the physics and the mathematics of CT and cannot be eliminated (see 7.6). Others are due to hardware or software deficiencies in the design and can be eliminated by improved engineering.

5.3.3.2 The type and severity of artifacts are two of the factors that distinguish one CT system from another with otherwise identical specifications. The user must understand the differences in these artifacts and how they will affect the determination of the variables to be measured. For instance, absolute density measurements will be affected severely by uncompensated cupping, but radial cracks can be visible with no change in detectability.

6. Apparatus

6.1 Modern CT systems, both industrial and medical, are composed of a number of subsystems, typically those shown in Fig. 3. The choice of components for these subsystems depends on the specific application for which the system was designed; however, the function served by each subsystem is common in almost all CT scanners. These subsystems are:

6.1.1 An operator interface,
6.1.2 A source of penetrating radiation,
6.1.3 A radiation detector or an array of detectors,
6.1.4 A mechanical scanning assembly,
6.1.5 A computer system,
6.1.6 A graphical display system, and
6.1.7 A data storage medium.

6.2 *Operator Interface*—The operator interface defines what control the operator has over the system. From the perspective of the user, the operator interface is the single most important subsystem. The operator interface ultimately determines everything from the ease of use to whether the system can perform

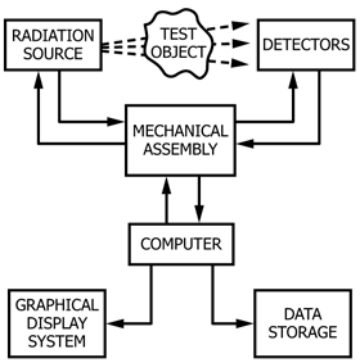

FIG. 3 Typical Components of a Computed Tomography (CT) System

repetitive scan sequences. In short, the operator interface determines how the system is used.

6.3 *Radiation Sources*—There are three rather broad types of radiation sources used in industrial CT scanners: (*1*) X-ray tubes, (*2*) linear accelerators, and (*3*) isotopes. The first two broad energy spectra are (polychromatic or bremsstrahlung) electrical sources; the third is approximately monoenergetic radioactive sources. The choice of radiation source is dictated by precisely the same rules that govern the choice of radiation source for conventional radiographic imaging applications. A majority of existing CT scanners use electrical bremsstrahlung X-ray sources: X-ray tubes or linear accelerators. One of the primary advantages of using an electrical X-ray source over a radioisotope source is the much higher photon flux possible with electrical radiation generators, which in turn allows shorter scan times. The greatest disadvantage of using an X-ray source is the beam hardening effect associated with polychromatic fluxes. Beam hardening results from the object preferentially absorbing low-energy photons contained in the continuous X-ray spectrum. Most medical scanners use for a source an X-ray tube operating with a potential of 120 to 140 kV. Industrial scanners designed for moderate penetrating ability also use X-ray tubes, but they usually operate at higher potentials, typically 200 to 400 kV. Systems designed to scan very massive objects, such as large rocket motors, use high-energy bremsstrahlung radiation produced by linear accelerators. These sources have both high flux and good penetration, but they also have a broad continuous spectrum and the associated beam-hardening effect. Isotope sources are attractive for some applications. They offer an advantage over X-ray sources in that problems associated with beam hardening are nonexistent for the monoenergetic isotopes such as Cesium-137 and Cobalt-60. They have the additional advantages, which are important in some applications, that they do not require bulky and energy-consuming power supplies, and they have an inherently more stable output intensity. The intensity of available isotopic sources, however, is limited by specific activity (photons/second/gram of material). The intensity affects signal-to-noise ratio, and, even more importantly, the specific activity determines source spot size and thus spatial resolution. Both of these factors tend to limit the industrial application of isotopic scanners. Nevertheless, they can be used in some applications in which scanning time or resolution is not critical.

6.4 *Radiation Detectors*—A radiation detector is used to measure the transmission of the X-rays through the object along the different ray paths. The purpose of the detector is to convert the incident X-ray flux into an electrical signal, which can then be handled by conventional electronic processing techniques. The number of ray sums in a projection should be comparable to the number of elements on the side of the image matrix. Such considerations result in a tendency for modern scanners to use large detector arrays that often contain several hundred to over a thousand sensors.

6.4.1 *Scintillation Detectors*—This type of transducer takes advantage of the fact that certain materials possess the useful property of emitting visible radiation when exposed to X-rays. By selecting fluorescent materials that scintillate in proportion to the incident flux and coupling them to some type of device that converts optical input to an electrical signal, sensors suitable for CT can be engineered. The light-to-electrical converter is usually a photodiode or photomultiplier tube, but video-based approaches are also widely employed. Like ionization detectors, scintillation detectors afford considerable design flexibility and are quite robust. Scintillation detectors are often used when very high stopping power, very fast pulse counting, or areal sensors are needed. Recently, for high-resolution CT applications, scintillation detectors with discrete sensors have been reported with array spacings on the order of 25 μm. Both ionization and scintillation detectors require considerable technical expertise to achieve performance levels acceptable for CT.

6.5 *Mechanical Scanning Equipment*—The mechanical equipment provides the relative motion between the test article, the source, and the detectors. It makes no difference, at least in principle, whether the test object is moved systematically relative to the source and detectors, or if the source and detectors are moved relative to the test object. Physical considerations such as the weight or size of the test article should be the determining factors for the most appropriate motion to use.

6.5.1 The majority of scan geometries that have been employed can be classified as one of the following four generations. This classification is a legacy of the early, rapid development of CT in the medical arena and is reviewed here because these terms are still widely used. The distinctions between these early scan geometries are illustrated in Fig. 4.

6.5.1.1 First-generation CT systems are characterized by a single X-ray source and single detector that undergo both linear translation and rotational motions. The source and detector assembly is translated in a direction perpendicular to the X-ray beam. Each translation yields a single view, as shown in Fig. 2. Successive views are obtained by rotating the test article and translating again. The advantages of this design are simplicity, good view-to-view detector matching, flexibility in the choice

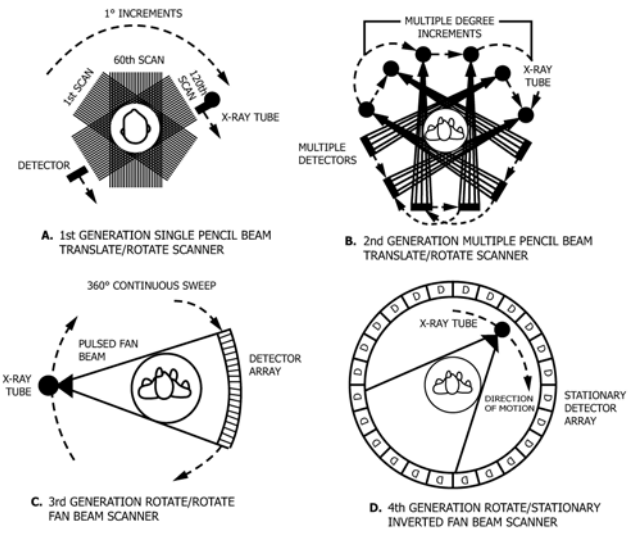

FIG. 4 Four Sketches Illustrating the Evolution of Medical CT Scan Geometries. Each Embodiment is Representative of a Distinct Generation of Instrumentation

of scan parameters (such as resolution and contrast), and ability to accommodate a wide range of different object sizes. The disadvantage is a longer scanning time.

6.5.1.2 Second-generation CT systems use the same translate/rotate scan geometry as the first generation. The primary difference is that second-generation systems use a fan beam of radiation and multiple detectors so that a series of views can be acquired during each translation, which leads to correspondingly shorter scan times. Like first-generation systems, second-generation scanners have the inherent flexibility to accommodate a wide range of different object sizes, which is an important consideration for some industrial CT applications.

6.5.1.3 Third-generation CT systems normally use a rotate-only scan geometry, with a complete view being collected by the detector array during each sampling interval. To accommodate objects larger than the field of view subtended by the X-ray fan, it is possible to include part translations in the scan sequence, but data are not acquired during these translations as during first- or second-generation scans. Typically, third-generation systems are faster than their second-generation counterparts; however, because the spatial resolution in a third-generation system depends on the size and number of sensors in the detector array, this improvement in speed is achieved at the expense of having to implement more sensors than with earlier generations. Since all elements of a third-generation detector array contribute to each view, rotate-only scanners impose much more stringent requirements on detector performance than do second-generation units, where each view is generated by a single detector.

6.5.1.4 Fourth-generation CT systems also employ a rotate-only scan motion. The difference between third-generation and fourth-generation systems is that a fourth-generation CT system uses a stationary circular array of detectors and only the source moves. The test specimen is placed within the circle of detectors and is irradiated with a wide fan beam which rotates around the test article. A view is made by obtaining successive absorption measurements of a single detector at successive positions of the X-ray source. The number of views is equal to the number of detectors. These scanners combine the artifact resistance of second-generation systems with the speed of third-generation units, but they can be more complex and costly than first-, second-, or third-generation machines, they require that the object fit within the fan of X-rays, and they are more susceptible to scattered radiation.

6.5.1.5 Several other CT scanner geometries that have been developed and marketed do not precisely fit the above categories. However, there is no agreed-upon generation designation for them.[4]

(1) The cine CT system has no mechanical scanning motion. In this system both the X-ray detector and the X-ray tube anode are stationary. The anode, however, is a very large semicircular ring that forms an arc around the Object scan circle, and is part of a very large, non-conventional X-ray tube. The source of X-rays is moved around the same path as a fourth generation CT scanner by steering an electron beam around the X-ray anode. The detectors are positioned opposite the source circle and full rotational scans are created without the need for object or system motion. Because the electron beam can be moved very rapidly, this scanner can attain very rapid image acquisition rates. This system has been referred to variably as fifth generation and sixth generation. It has also been described as a stationary-stationary scanner. The terms millisecond CT, ultrafast CT and electron beam CT have also been used, although the latter can be confusing since the term suggests that the object is exposed to an electron beam.

(2) In volume CT, a cone beam or highly-collimated, thick, parallel beam is used rather than a fan beam, and a planar grid replaces the linear series of detectors. This allows for much faster data acquisition, as the data required for multiple slices can be acquired in one rotation. It is computationally more intensive (although high speed computers are now making this approach practical) and corrections for scatter and hardening effects may be required for sufficient image quality. Large cone beam angles may lead to unsharpness at the outer volume elements.

6.5.2 A significant factor in driving medical CT systems to use rotate-only scan geometries was the requirement that scanning times be short compared to the length of time that a patient can remain motionless or that involuntary internal motion can be ignored (that is, seconds). These considerations are not as important for industrial applications in which scan times for specific production-related items can typically be much longer (that is, minutes) and the dose to the object is often not an important factor. A second-generation scan geometry is attractive for industrial applications in which a wide range of part sizes must be accommodated, since the object does not have to fit within the fan of radiation as it generally does with third- or fourth-generation systems. A third-generation scan geometry is attractive for industrial applications in which the part to be examined is well defined and scan speed is important. To date, first- and fourth-generation scan geometries have seen little commercial application, but there may be special situations for which they would be well suited. The ability of CT to image and quantify internal features makes it the nondestructive examination method of choice for inspecting parts containing complex internal structures or having various internal layers. When 100 %, or a large area, of a part needs to be inspected using CT, the most economical approach would be to use a volumetric CT system employing an area detector, assuming the desired image quality and uniformity can be obtained.

6.6 *Computer Systems*—The computer system(s) performs two major tasks: (*1*) controlling the scan motion, source operation, and data acquisition functions; and (*2*) handling the reconstruction, image display and analysis, and data archival and retrieval functions.

6.7 *Image Display and Processings*—Image display and processing are subfunctions of the computer system that provide a degree of image interaction not available with conventional radiography. The mapping between the pixel linear attenuation coefficient and the displayed intensity of the pixel can be changed to accommodate the best viewing conditions for a particular feature. Image processing functions

[4] Medcyclopaedia.com: GE Healthcare, Bio-Sciences, Europe.

such as statistical and densitometric analyses can be performed on an image or group of images. The digital nature of the image allows major advances in the way data are processed, analyzed, and stored. This process of mapping reconstructed pixel values to displayed pixel values is shown in Fig. 5.

6.8 *Archival Data Storage*—Information such as image data, operating parameters, part identification, operator comments, slice orientation, and other data is usually saved (archived) in a computer-readable, digital format on some type of storage medium. The advantage of saving this material in computer-readable format rather than in simple hardcopy form is that it would take dozens of pictures of each slice at different display conditions to approximate the information contained in a single CT image. Also, images of samples made with old and new data sets can be compared directly, and subsequent changes in reconstruction or analysis procedures can be reapplied to saved data or images.

6.9 These elements are the basic building blocks of any CT system. Each CT system will have its own particular set of features. It is the responsibility of the user to understand these differences and to select the system most appropriate for the intended application.

7. Theoretical Background

7.1 *Background*—This section will cover the theoretical background associated with CT. First, the means of penetrating radiation interaction will be discussed. Second, the specifics of CT will be delineated.

7.2 *X-Ray Interactions*—Penetrating radiation is classified according to its mode of origin. Gamma rays are produced by nuclear transitions and emanate from the atomic nucleus. Characteristic X-rays are produced by atomic transitions of bound electrons and emanate from the electronic cloud. Continuous X-rays, or bremsstrahlung, are produced by the acceleration or deceleration of charged particles, such as free electrons or ions. Annihilation radiation is produced by the combination of electron-positron pairs and their subsequent decomposition into pairs of photons. All evidence suggests that the interaction of these photons with matter is independent of their means of production and is dependent only on their energy. For this reason, this document refers to penetrating radiation in the energy range from a few keV to many MeV as X-rays, regardless of how they are produced.

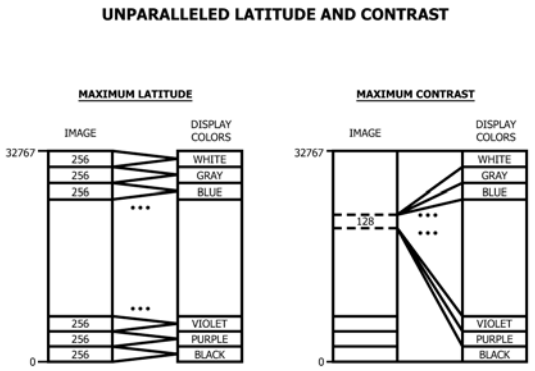

FIG. 5 Conceptual Illustration of the Process of Mapping a Large Range of Image Values Onto a Much Smaller Range of Displayable Values. Two Important Cases are Shown: the One on the Left Illustrates the Case of Maximum Image Latitude; the One on the Right Illustrates the Case of Maximum Contrast Over a Narrow Range of Contrast

7.2.1 X-rays can in theory interact with matter in only four ways: they can interact with atomic electrons; they can interact with nucleons (bound nuclear particles); they can interact with electric fields associated with atomic electrons, or atomic nuclei, or both; or they can interact with meson fields surrounding nuclei. In theory, an interaction can result in only one of three possible outcomes: the incident X-ray can be completely absorbed and cease to exist; the incident X-ray can scatter elastically; or the incident X-ray can scatter inelastically. Thus, in principle, there are twelve distinct ways in which photons can interact with matter (see Fig. 6). In practice, all but a number of minor phenomena can be explained in terms of just a few principal interactions; these are highlighted in Fig. 6. Some of the possible interactions have yet to be physically observed.

7.2.2 The photon-matter interactions of primary importance to radiography are the ones which dominate observable phenomenon: photoelectric effect, Compton scattering, and pair production. Their domains of relative importance as a function of photon energy and material atomic number are shown in Fig. 7. At energies below about 1 MeV, pair production is not allowed energetically; and X-ray interactions with matter are dominated by processes involving the atomic electrons. Of the other possible interactions (see Fig. 6), Rayleigh scattering is typically small but non-negligible; the rest are either energetically forbidden or insignificant. At energies above 1 MeV, pair production is energetically allowed and competes with Compton scattering. Of the other possible interactions, photodisintegration is typically negligible in terms of measurable attenuation effects, but at energies above about 8 MeV can lead to the production of copious amounts of neutrons. The rest of the interactions are either energetically forbidden or insignificant.

7.2.3 The three principle interactions are schematically illustrated in Fig. 8. With the photoelectric effect (see Fig. 8), an incident X-ray interacts with the entire atom as an entity and is completely absorbed. To conserve energy and momentum, the atom recoils and a bound electron is ejected. Although the subsequent decay processes lead to the generation of characteristic X-rays and secondary electrons, these are not considered part of the photoelectric effect. As can be seen in Fig. 7, the photoelectric effect predominates at low energies. Photoelectric absorption depends strongly upon atomic number, varying approximately as z raised to the 4^{th} or 5^{th} power.

7.2.4 With Compton scattering (see Fig. 8), an incident X-ray interacts with a single electron (which, practically speaking, is almost always bound) and scatters inelastically, meaning the X-ray loses energy in the process. This type of scattering is often referred to as incoherent scattering, and the terms are used interchangeably. To conserve energy and momentum, the electron recoils and the X-ray is scattered in a different direction at a lower energy. Although the X-ray is not absorbed, it is removed from the incident beam by virtue of having been diverted from its initial direction. The vast

Effects of Interaction	Atomic Electrons	Nucleons	Electric Field Of Atom	Meson Field Of Nucleus
Complete Absorption	Photoelectric Effect	Photo Disintegration	Pair Production	Meson Production
Elastic Scattering	Rayleigh Scattering	Thomson Scattering	Delbruck Scattering	Not Observed
Inelastic Scattering	Compton Scattering	Nuclear Resonance Scattering	Not Observed	Not Observed

Jannafl/Bechtel54/4-95

FIG. 6 X-Ray Interactions with Matter

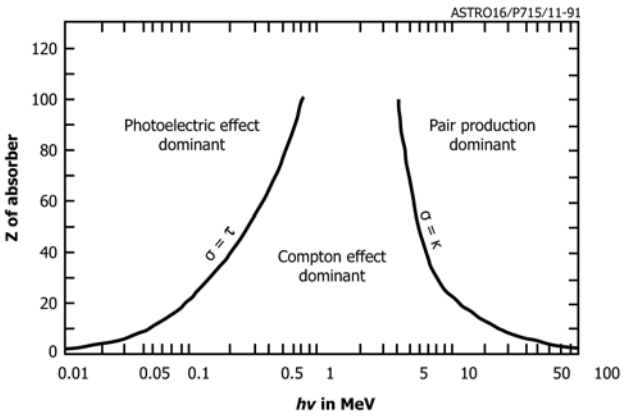

FIG. 7 Principal X-Ray Interactions

majority of background radiation in and around radiographic equipment is from Compton-scattered X-rays. As can be seen in Fig. 7, Compton scattering predominates at intermediate energies and varies directly with atomic number per unit mass.

7.2.5 With pair production (see Fig. 8), an incident X-ray interacts with the strong electric field surrounding the atomic nucleus and ceases to exist, creating in the process an electron-positron pair. Energy and momentum are conserved by the emerging pair of particles. Although the positrons eventually interact with electrons, generating annihilation radiation, this secondary effect is not considered part of the pair production process. As can be seen in Fig. 7, pair production predominates at high energies. Pair production varies approximately with atomic number as $z\ (z + 1)$.

7.3 *CT Technical Background*—CT is the science of recovering an estimate of the internal structure of an object from a systematic, nondestructive interrogation of some aspect of its physical properties. Generally, but not always **(2)**, the problem is kept manageable by limiting the task to a determination of a single image plane through the object. If three-dimensional information is required, it is obtained by comparing and, if necessary, resectioning **(3)** contiguous cross-sections through the object of interest.

7.3.1 In its most basic form, the CT inspection task consists of measuring a complete set of line integrals involving the physical parameter of interest over the designated cross-section and then using some type of computational prescription, or algorithm, to recover an estimate of the spatial variation of the parameter over the desired slice. In order to best illustrate the basic principles of CT, the discussion limits itself to the examination problem of determining a single image plane through an object. Separate sections focus on (*1*) what constitutes an acceptable CT data set, (*2*) one way in which such a data set can be collected, and (*3*) some of the competing effects that limit performance in practice. The discussion of the companion task of image reconstruction limits itself to the problem of reconstructing a single two-dimensional image; three-dimensional reconstructions are not discussed. The treatment includes the goal of the reconstruction process and one way in which CT data can be reconstructed.

7.3.2 The task of obtaining a usable data set is reviewed in 7.4 – 7.6. The companion problem of how these data are then reconstructed to produce an image of the object is reviewed in 7.7 and 7.8.

7.4 *Radon Transform*—The theoretical mathematical foundation underlying CT was established in 1917 by J. Radon **(4)**. Motivated by certain problems of gravitational physics, Radon established that if the set of line integrals of a function, which is finite over some region of interest and zero outside it, is known for all ray paths through the region, then the value of the function over that region can be uniquely determined. A particular function and its associated set of line integrals form a transform pair; the set of integrals is referred to as the Radon transform of the function. Radon demonstrated the existence of an inverse transform for recovering a function from its Radon transform, providing an important existence theorem for what later came to be called CT. Over the years, the process of recovering a function from its Radon transform has been rediscovered numerous times **(5-9)**.

7.4.1 In a classic example of the old principle that "like equations have like solutions," tomography has been demonstrated using many different physical modalities to obtain the necessary line integrals of some physical parameter. Objects ranging in size from bacteriophages **(10)** to supernova **(11)** have been studied tomographically using a wide variety of physical probes, including X-rays (medical CAT scanners or simple X-ray CT) **(12, 13)**, sound waves (ultrasonic imaging) **(14, 15)**, electromagnetic fields (NMR, or, more commonly now, MR imaging) **(16)**, ionizing particles **(17, 18)**, and biologically active isotopes (SPECT and PET scanners) **(19-21)**. These methods have been used to study many types of material properties, such as X-ray attenuation, density, atomic number, isotopic abundance, resistivity, emissivity, and, in the case of living specimens, biological activity.

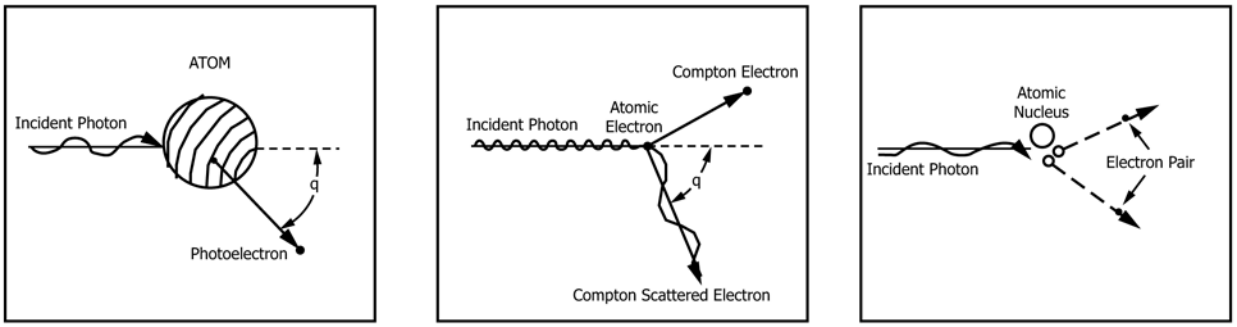

FIG. 8 X-Ray Interaction Mechanisms

7.4.2 The essential technological requirement, and that which these various methods have in common, is that a set of systematically sampled line integrals of the parameter of interest be measured over the cross-section of the object under inspection and that the geometrical relationship of these measurements to one another be well known. Within this constraint, many different methods of collecting useful data exist, even for the same imaging modality. However, the quality of the resulting reconstruction depends on at least three major factors: (*1*) how finely the object is sampled, (*2*) how accurately the individual measurements are made, and (*3*) how precisely each measurement can be related to an absolute frame of reference.

7.5 *Sampling the Radon Transform*—Given this general background, the discussion here now focuses on the specific task of tomographic imaging using X-rays as the inspection modality. For monoenergetic X-rays, attenuation in matter is governed by Lambert's law of absorption (**22**), which holds that each layer of equal thickness absorbs an equal fraction of the radiation that traverses it. Mathematically, this can be expressed as the following:

$$\frac{dI}{I} = -\mu dx \tag{1}$$

where:

I = the intensity of the incident radiation,
dI/I = the fraction of radiation removed from the flux as it traverses a small thickness, dx, of material, and
μ = the constant of proportionality.

In the physics of X-ray attenuation, μ is referred to as the linear absorption coefficient. Eq 1 can be integrated easily to describe X-ray attenuation in the following perhaps more familiar form (**1**):

$$I = I_o e^{-\mu x} \tag{2}$$

where:

I_o = the intensity of the unattenuated radiation, and
I = the intensity of the transmitted flux after it has traversed a layer of material of thickness x.

7.5.1 If X-rays penetrate a non-homogeneous material, Eq 2 must be rewritten in the more general form:

$$I = I_o e^{-\int \mu(s) ds} \tag{3}$$

where the line integral is taken along the direction of propagation and μ(*s*) is the linear absorption coefficient at each point on the ray path. In X-ray CT, the fractional transmitted intensity, I/I_o, is measured for a very large number of ray paths through the object being inspected and is then logged to obtain a set of line integrals for input to the reconstruction algorithms. Specifically, the primary measurements, I and I_o, are processed, often "on the fly," to obtain the necessary line integrals:

$$\int \mu(s) ds = -ln(I/I_o) \tag{4}$$

7.5.2 To obtain an adequate measure of the line integrals, highly collimated pencil beams of X-rays are used to make the measurements of the fractional transmittance. In the terminology of CT, the set of line integrals resulting from a scan of an object can be grouped conceptually into subsets referred to as views. Each view corresponds to a set of ray paths through the object from a particular direction (see Fig. 9). The views are also referred to as projections or profiles, while each individual datum within a given projection is referred to as a sample or often simply a data point.

7.5.3 As previously indicated, the reconstruction problem places a number of severe constraints on the data. First, the set of line integrals must represent a systematic sampling of the entire object. If the circle of reconstruction is inscribed in an M by M image matrix, this implies $(\pi/4)\ M^2$ unknowns and a need for at least $(\pi/4)\ M^2$ linearly independent measurements. Refs (**23-25**) have examined the minimum number of views and samples per view necessary to reconstruct an arbitrary object from data in which the dominant source of noise is photon statistics. Since the presence of random noise corrupts the data, one would expect the minimum sampling requirements to be greater than they are for noise-free data as well as to be

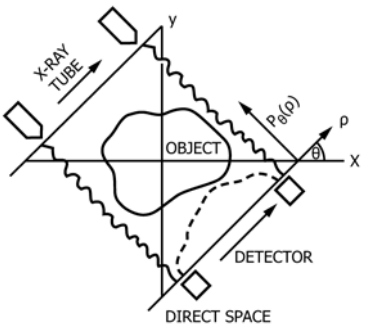

FIG. 9 Schematic Illustration of Basic CT Scan Geometry Showing a Single Profile Consisting of Many Discrete Samples

sensitive to the algorithm employed. Surprisingly, most algorithms in use today can provide stable, high-quality reconstructions for data sets approaching the theoretical minimum sampling requirements. Typically, data set sizes are on the order of one to three times the minimal amount, depending on the system and the application. Arbitrarily complex objects require more data than objects with simple geometrical shapes or highly developed symmetries.

7.5.4 The number of views and samples needed depends on the approach used and the amount of data required; however, independent of approach, the number of samples per view is generally more important than the number of views, and the relative proportion of views and samples should reflect this principle. Predicting the amount of noise in a CT image reconstructed with an adequate number of samples and views is a well-studied problem (**23-26**); predicting the amount of noise when an insufficient number of samples or views, or both, is used is more difficult and less well studied (**24, 27**).

7.5.5 Second, each line integral must be accurately known. It has been found that errors in the measurement of the fractional transmittance of even a few tenths of one percent are significant (**28**). This places strict requirements on the data acquisition system. As a result, the radiation detectors used in standard X-ray CT systems, along with their associated electronics, represent some of the most sophisticated X-ray sensor technology developed to date. A typical CT system can handle a dynamic range (the ratio of peak signal-strength-to-rms noise) on the order of a million-to-one (**29, 30**), with a linearity of better than 0.5 % (**30, 31**).

7.5.6 Third, each sample must be referenced accurately to a known coordinate system. It is useless to have high-precision transmission measurements if the exact ray path through the object to which it corresponds is unknown. This places strict demands on the mechanical equipment. Studies have shown that the angle of each view must be known to within a few hundredths of a degree, and the linear position of each sample within a given projection must be known to within a few tens of micrometres (**28**).

7.5.7 CT equipment has evolved to the stage at which each of these performance requirements can be reasonably well satisfied. A state-of-the-art scanner routinely collects millions of measurements per scan, with each one quantified accurately and referenced precisely to a specific line-of-sight through the object of interest. Once collected, the data are then passed to the reconstruction algorithm for processing.

7.6 *Physical Limitations on the Sampling Process*—The quality of the reconstructed image depends on the quality of the data generated by the scanner. In actual practice, equipment and methods are limited in their ability to accurately estimate line integrals of the attenuation through an object (**32**). Some of the more prominent sources of inaccuracy are the following: photon statistics, beam hardening, finite width of the X-ray pencil beams, scattered radiation, and electronic and hardware nonlinearities or instabilities, or both. Considerable attention is devoted to managing these problems.

7.6.1 The penetrating radiation used by CT systems is produced in a number of ways, all of which involve random atomic or subatomic processes, or both. The probability of any one atom participating at any given moment in time is remote, but the sheer numbers of atoms typically involved guarantees a finite emission rate. The number of photons produced per unit time varies because of the statistical nature of the radiation emission process. The variations have well-defined characteristics, which can be described by what are referred to mathematically as Poisson statistics. This ubiquitous radiographic problem of photon statistics is handled in CT by integrating (or counting) long enough to keep statistical noise to a diagnostically acceptable level (**27, 33**). What constitutes an acceptable noise level is defined by the application and can vary widely.

7.6.2 Beam hardening is a problem encountered with polychromatic X-ray sources, such as X-ray tubes or linear accelerators (linacs). Such bremsstrahlung sources, as opposed to monoenergetic (that is, isotopic) sources, produce a flux whose average radiation energy becomes progressively higher as it propagates through an object because the lower-energy photons are preferentially absorbed with respect to the more energetic ones. This effect compromises the validity of Eq 4 since μ is no longer associated with a single energy but rather with an effective energy that is constantly changing along the ray path. Although this effect can be partially controlled by conscious engineering choices, it is generally a significant problem and must be corrected for at some stage in the reconstructive processing (see Refs (**34-36**) and references therein).

7.6.3 Another source of difficulties is with the finite width of the individual pencil beams. A pencil beam of X-rays is geometrically defined by the size of the focal spot of the X-ray source and the active area of each detector element. Because these are finite, each source-detector line-of-sight defines a thin strip rather than an infinitely thin mathematical line. As a result, each measurement represents a convolution of the desired line integral with the profile of the pencil beam. In general, the width of the strip integrals is small enough that although some loss of spatial information occurs, no distracting artifacts are generated. The exception occurs when there are sharp changes in signal level. The error then becomes significant enough to produce artifacts in the reconstructed image which manifest themselves in the form of streaks between high-contrast edges in the image. These edge artifacts (**32, 37-39**) are caused by the mathematical fact that the logarithm of the line integral convolved with the profile of the pencil beam (which is what is measured) does not equal the convolution of the beam profile with the logarithm of the line integral (which is what the reconstruction process desires).

7.6.4 Unfortunately, edge artifacts cannot be eliminated by simply reducing the effective size of the focal spot or the detector apertures, or both, through judicious collimation. As the strip integrals are reduced to better approximate line integrals and reduce susceptibility to edge artifacts, count rates become severely curtailed, which leads to either much noisier images or much longer scan times, or both. In practice, the pencil beams are engineered to be as small as practicable, and if further reductions in edge-artifact content are required, these are handled in software. However, software corrections entail some type of deconvolution procedure to correct for the beam

profile (32, 37-39) and are complicated by the fact that the intensity profile of the pencil beam has a complex geometrical shape that varies along the path of the X-rays.

7.6.5 The same problem occurs when the structure of the object undergoing inspection changes rapidly in the direction normal to the plane of the scan. When the change is sizeable over the thickness of the slice, the same mathematics that lead to the edge artifact produce what in this case is commonly referred to as a partial-volume artifact (32, 37-39). It manifests itself as an apparent reduction in attenuation coefficient in those parts of the image where the transverse structure is changing rapidly. In the absence of *a priori* information, nothing is known about the spatial variation of object structure within the plane of the scan, and software corrections are much more difficult to implement.

7.6.6 Still another source of problems arises from the presence of scattered radiation. When multiple detector elements are employed, there is always the chance that radiation removed from the incident flux by Compton interactions will be registered in another detector. This scattered radiation, which becomes more severe with higher energies, cannot be easily distinguished from the true signal and corrupts the measurements. This problem can be reduced (40), but not eliminated, through the use of proper collimation.

7.6.7 The last type of inaccuracy is electronic and mechanical nonlinearities and instabilities. These may result from correctable engineering deficiencies or basic physical limitations of the available components. The validity of the data is compromised in either case. In some cases, the problem can be corrected (or reduced) in software; in others, it can be fixed only by reengineering the offending subsystem. Because the bulk of existing information on this crucial topic is commercially sensitive and therefore proprietary, the literature is relatively sparse. All that can be said on these issues here is that considerable effort is required to keep these types of errors small compared to other less manageable sources of error, such as those discussed above.

7.7 *Inverting the Radon Transform*—The reconstruction task can be defined as follows: given a set of systematic transmission measurements corrupted by various known and unknown sources of error, determine the best estimate of the cross-section of the object associated with that data. Cormack (8) and, earlier, Radon (4) showed that it is possible to "find a real function in a finite region of a plane given its line integrals along all straight lines intersecting the region." Cormack later extended this result in a companion paper (41) that described "a method for determining a variable gamma-ray absorption coefficient in a sample from (a finite set of) measurements made outside the sample." Although Cormack's algorithm never lent itself well to digital processing, at the time it provided a valuable existence theorem: it was possible to recover a useful estimate of the internal structure of an object from a finite number of measurements of the X-ray transmission through an object of interest.

7.7.1 Over time, a large number of methods (that is, algorithms) for recovering an estimate of the cross-section of an object (that is, reconstructing a CT image) from its Radon transform (that is, the set of measurements of the fractional transmittance) have evolved. They can be grouped broadly into three classes of algorithms: (*1*) matrix inversion methods, (*2*) finite series-expansion methods, and (*3*) transform methods. The general features of each are described in 7.7.2 – 7.7.8.

7.7.2 Matrix inversion methods follow naturally from a very direct approach to the problem of reconstructing an M by M image matrix. At the outset, an M by M matrix consists of a blank matrix of M^2 unknown attenuation values; while, on the other hand, each measurement can be described in terms of a linear combination of some fraction of these unknown attenuation values. Thus, from elementary algebraic considerations, a set of M^2 linearly independent measurements can in principle be solved for the unknown attenuation values. Further, because a set of linear equations can be solved very generally using matrices, one class of algorithms focuses on matrix methods (42).

7.7.3 Unfortunately, solving for N unknowns using matrices involves determining and inverting an N by N matrix. If N is a large number, such as M^2, the size of the matrix and the inversion task becomes completely intractable with current computer technology. This is not to say that matrix inversion methods are not valuable, but that they should not be judged on the basis of contemporary commercial merits. Basic research in this area is an ongoing enterprise and provides valuable insight into CT problems (24). However, such methods must await the further evolution of computer technology to make their way into commercial CT systems.

7.7.4 When the first CT instruments were introduced in the early 1970s, reconstructions were performed with what are now classified as finite series-expansion algorithms. The original EMI scanner invented by G. N. Hounsfield used such an approach (43). These methods, which included so-called algebraic reconstruction techniques (44), simultaneous iterative reconstruction techniques (45, 46), and maximum entropy algorithms (47, 48), are rooted in a completely different branch of mathematics from the transform methods described next. Stated simply, these methods iteratively alter the reconstruction matrix until a grid of values is obtained which produces line integrals that match the measured data as nearly as possible. Obviously, a large number of figures of merit can be used to determine what constitutes the best match, given the statistical fluctuations in the data; in addition, great latitude exists in the implementation of the iterative procedure (see Ref (42) and references therein).

7.7.5 While commercial CT systems no longer use iterative methods because of their inherent slowness, they offer numerous advantages that suggest they could experience a rebirth of popularity as computer technology continues to develop: they can be adapted readily to a far broader range of physical modalities and geometries (see, for instance, Refs (49) and (50)), they are reported to be less susceptible to edge artifacts (51), they are the preferred method for handling the complex reconstruction problems of emission CT (18, 52, 53), they are the best way of dealing with limited-angle data (48) or underdetermined data (too few views or samples) (54, 55), and they can be used when full three-dimensional reconstructions

are performed (**56, 57**), as opposed to merely stacking adjacent slices. (See the review article by Censor (**42**) for further information.)

7.7.6 Transform methods, the third class of restorative algorithms, are based on analytical inversion formulas. Because they are easy to implement, are fast in comparison to the other methods, and can produce high-quality images, they are universally used by commercial CT systems. The two primary types of transform methods are (*1*) the convolution-backprojection algorithm (**58-60**) and (*2*) the direct Fourier algorithm (**4, 61**), but the so-called ρ-filtered layergram method has also been used in special situations (**62**). They are based on the underlying fact that the one-dimensional Fourier transform of a CT projection of an object corresponds to a spoke in Fourier space of the two-dimensional transform of that object (the so-called Central-Section Theorem or Projection-Slice Theorem (**63**)). Thus, in theory, all that is required in order to obtain an image by this method is to transform each projection as it is collected; place it along its proper spoke in two-dimensional Fourier space; and when all the views have been processed, take the inverse two-dimensional Fourier transform to obtain the final image. This method is called the direct Fourier transform algorithm.

7.7.7 Within this general framework, there is considerable latitude concerning which of the steps to conduct in Fourier space and which to conduct in direct space. The advantages of each must be weighed against the disadvantages. The direct Fourier algorithm is potentially the fastest method; however, due to interpolation problems, X-ray CT images have not yet been reported with the same quality as those obtained with the convolution-backprojection method (**61, 63, 64**). Although some recent work has showed promising results (**65**), direct Fourier techniques are used primarily in applications that collect Fourier transforms of the projections directly, such as radio astronomy and magneticresonance (MR) imaging (**66, 67**). The convolution-backprojection method (or its twin, the filtered-backprojection method) is theoretically not as fast as the direct Fourier method, but it produces excellent images and with special-purpose hardware is capable of acceptable reconstruction times. The ρ-filtered layergram is impracticable when dealing with large amounts of digital data (a deficiency that eliminates its use in commercial CT systems) but has the virtue of lending itself nicely to optical implementation (**68, 69**), a technique that could someday be used to process most CT data. These methods are reviewed, along with several tutorials, in the article by Lewitt (**63**).

7.7.8 For the sake of completeness, it should be mentioned that there is also a small class of reconstruction algorithms that are a hybrid of transform and series-expansion methods and hence do not fit logically into either of these two broad groups. Some examples are described in Ref (**63**).

7.8 *Convolution-Backprojection Methods*—In order to give the user a more intuitive feeling for the reconstruction process, the convolution-backprojection algorithm is described. It is provided to give a sense of how such large amounts of data can be processed efficiently into a high-quality image. No effort is made to be mathematically rigorous; the interested reader is referred to Ref (**70**) for a particularly readable account and to Ref (**63**) for a more detailed, but still lucid, treatment of this algorithm.

7.8.1 First, consider the sequence of steps shown in Fig. 10. Frame A shows a point object being scanned and the idealized response of a single detector as it traverses the field of view. Frame B shows each of the many profiles collected during this scan backprojected across an initially blank circle of reconstruction. Backprojection can be thought of as reversing the data collection process. Each sample within a given projection represents the fractional transmittance of a narrow beam of X-rays through the object, which is assumed to be sufficiently well approximated by small, discrete pixels of constant attenuation. During backprojection, the value of each sample in the profile is numerically added to all of the image pixels that participated in the attenuation process for that sample. Conceptually, backprojection can be thought of as smearing each profile back across the image in the direction of the radiation propagation.

7.8.2 Frame C shows the net result of this operation. For a point object, the profiles superimpose to produce a central spike with a broad skirt that falls off as $1/r$ (at any radius, the number of backprojected rays radiating from the center is a constant). It is implicitly assumed here that a large number of

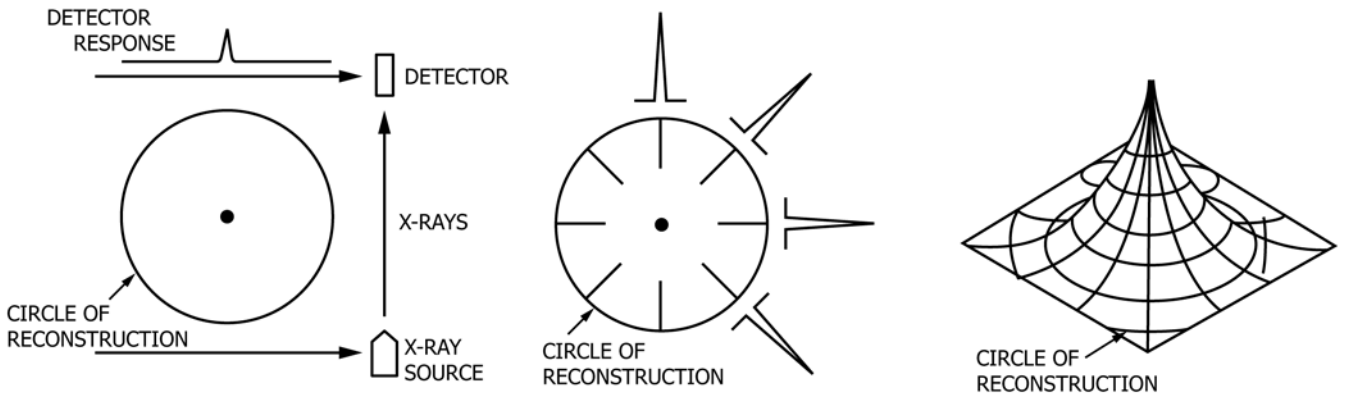

A. PROJECTION OF A POINT OBJECT **B.** NORMAL BACK PROJECTION TECHNIQUE **C.** RECONSTRUCTED IMAGE OF A POINT

FIG. 10 Straight Backprojection

profiles have been used; hence the smooth, featureless falloff. One of the earliest attempts at reconstruction used this approach (**6**). The product was a blurry but diagnostically useful image, at least in the absence, at that time, of a viable alternative.

7.8.3 Fig. 11 shows an improved version of this basic approach. Frame A shows the same scan situation depicted in Fig. 10. In Frame B, however, each profile has been convolved with a function that preserves the essential response of the detector to the presence of the point object but adds a negative tail to beat down the $1/r$ falloff that occurs with pure back-projection. The result of back-projecting these modified profiles is schematically illustrated in Frame C, where the point object is shown reconstructed in much sharper detail. This so-called convolution-back-projection method is the method used by virtually all commercial CT systems. It is easy to implement with digital techniques, is numerically robust, and is adaptable to special-purpose computer equipment, such as array processors or hardwired back-projectors.

7.8.4 To obtain an idea of how this appears mathematically, the results of Eq 4 are rewritten in the following form:

$$P(\theta, \rho) = -ln[I(\theta,\rho)/I_o] = \int \mu(x, y)\, ds \tag{5}$$

As before, I represents a single ideal measurement, but it has been rewritten to explicitly recognize that the detector is oriented with respect to the object at some angle, θ, and some position, ρ, as indicated in Fig. 9. I_o is the unattenuated signal level, $\mu(x, y)$ is the two-dimensional distribution of the linear attenuation coefficient of the object, and ds is an element of distance along the X-ray path through the object at angle θ and position ρ. The values of $I(\theta, \rho)$ are normalized to unity and logged to yield a set of estimated line integrals through the object, $P(\theta, \rho)$.

7.8.5 With this notation, the convolution-backprojection process schematically shown in Fig. 11 can be written as follows:

$$\mu(x, y) = \int_{o}^{\pi} \int_{-\infty}^{\infty} P(\theta, \rho) g(\rho - \eta) d\eta d\theta \tag{6}$$

where:

g = the convolution function of the shape-theoretical form:

$$g(r) = \frac{\pi^2}{2}\left(\frac{\delta(r)}{r} - \frac{1}{r^2}\right) \tag{7}$$

where:

$\delta(r)$ = the Dirac delta function.

There is an obvious problem with expressing $g(r)$ in this form when working with digital computers. A severe discontinuity exists near the origin where, loosely speaking, the delta function must in some way be attached to the $-1/r^2$ tail. However, this expression is presented only to give the reader an idea of the behavior of $g(r)$; the rigorous mathematics of how such functions are handled digitally in practice are treated in the literature (see Refs (**63**) and (**70**) and references therein).

7.8.6 In words, Eq 6 and Eq 7 say that $\mu(x, y)$ can be recovered from a complete set of line integrals, $P(\theta, \rho)$, by first convolving each projection with a special function, g (that is, the integral over η in Eq 6) and then backprojecting each convolved view to obtain the final image (that is, the integral over θ in Eq 6). Convolving the views with the function, g, given in Eq 7 accomplishes two tasks: (*1*) the first term is just the polar-coordinate version of the delta function and serves to preserve the basic profile of each view; and (*2*) the second term corrects for the blurring introduced by the back-projection algorithm. In CT terminology, if the convolution is conducted in direct space (that is, the inner integral in Eq 6 is evaluated directly), the method is called convolution-backprojection; if it is conducted in Fourier space (which is generally a much faster way to do it), the method is called filtered-backprojection. This distinction is frequently overlooked, and the two terms are often used interchangeably.

8. Interpretation of Results

8.1 *Technical Objectives*—The goal of a CT X-ray imaging system is to nondestructively produce internal images of objects with sufficient detail to detect crucial features. The task of the CT user is to specify the system that will satisfy a particular need and to verify that the specification is met. The visibility of a feature in a CT image depends on the difference in X-ray attenuation between the feature and its background, size of the feature, size of the background object, X-ray optics, number of samples collected, X-ray exposure, and numerous

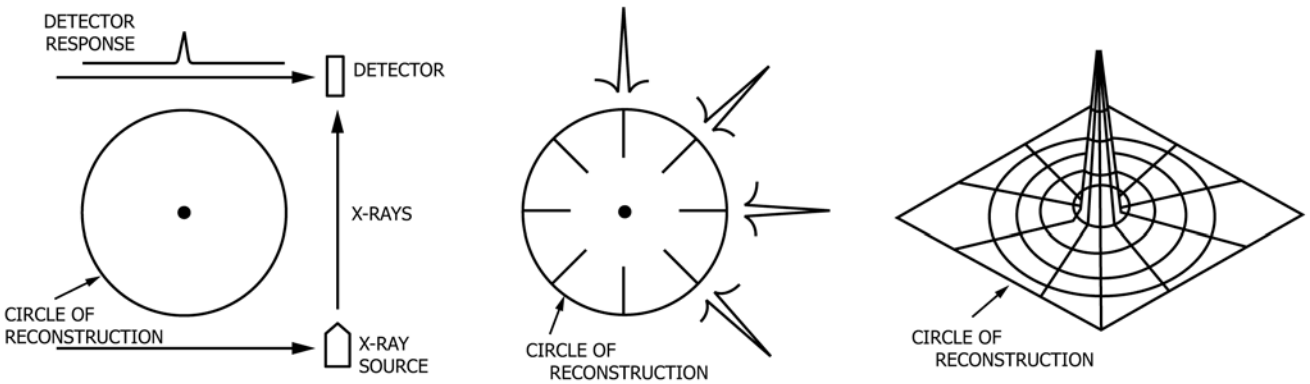

A. PROJECTION OF POINT OBJECT **B.** FILTERED BACK PROJECTION TECHNIQUE **C.** RECONSTRUCTION IMAGE OF A POINT

FIG. 11 Convolution Backprojection

other factors. To predict accurately the performance of a given system in specific application requires a very complicated modeling process. However, many researchers have shown that detectability obeys some fairly simple rules and can be expressed as a function of system noise, system resolution, size and composition of the background object, and size and composition of the feature.

8.1.1 It will be shown in the following sections how these rules can be used to help specify a CT system as well as how they can be used to verify a specification. First, some background is presented to help the user understand the roles of CT system resolution and noise in detectability. Contrast is defined in 8.2. The effect of system resolution on contrast is discussed in 8.3. The effect of system noise on contrast is discussed in 8.4. The findings of various researchers that relate contrast detectability (with a 50 % confidence level) to object size and system noise are presented in 8.5. The results of the previous sections are combined in 8.6 to aid the user in specifying a system for a particular need. The user is shown how to measure the performance of an existing system in 8.7.

8.2 *Contrast*—The quantity that is reconstructed in X-ray CT imaging is the linear attenuation coefficient, μ, usually within a two-dimensional slice defined by the thickness of the X-ray beam. It is measured in units of cm^{-1} and is directly proportional to the electron density of the material. To be distinguished, a feature must have a linear attenuation coefficient, μ_f, that is sufficiently different from the linear attenuation coefficient of its background material, μ_b.

8.2.1 Linear attenuation coefficients are functions of the incident X-ray energy, *E*. Fig. 12 shows the functional energy dependence of the X-ray linear attenuation coefficients of two hypothetical materials, μ_f and μ_b. It is seen that the degree of contrast, Δμ, between two materials varies greatly as a function of the energy. (For simplicity in these discussions, the X-rays used are assumed to have a single energy, *E*, or to be approximated by some mean energy, $\bar{E}$, if a spectrum of energies is used.) The X-ray energy is an important parameter that must be chosen for a given scan specification. It would seem advantageous to choose a low energy to maximize contrast; however, the attenuation coefficient is large for low energies, and this results in poor X-ray transmission and high system noise, which is detrimental to good detectability. Also, higher-energy systems usually have significantly higher X-ray flux than lower energy systems. The optimum tradeoff clearly depends, to a great extent, on the specific application.

8.2.2 Contrast in CT has been defined historically as the percent difference of a feature from a background material.

$$\text{Contrast, \%} = \frac{|\mu_f - \mu_b|}{\mu_b} \times 100\,\% \tag{8}$$

This expression has the disadvantage of being infinite for a feature in air, for which μ_b is effectively zero, but it is convenient for comparing the contrast of different materials in a given background. It should be noted that this definition for contrast assumes that the feature in question extends throughout the thickness of the CT slice. If the feature has thickness *h* but is imaged with a slice of larger thickness *t*, the contrast is further reduced by the factor *h/t*.

8.2.3 If the CT imaging system did not introduce degradation, a profile through the center of the feature shown in Fig. 13(a) would have the crisp shape shown in Fig. 13(b). Probability-distribution functions PDF(μ_f) and PDF(μ_b), which describe the probabilities of finding a given value μ inside the feature and inside the background, respectively, are plotted in Fig. 13(c). In the absence of degradation, only the value μ_b appears in the background, and only the value μ_f appears in the feature, with each normalized to unit probability. The contrast difference, Δμ, is simply given by:

$$\Delta\mu = |\mu_f - \mu_b| \tag{9}$$

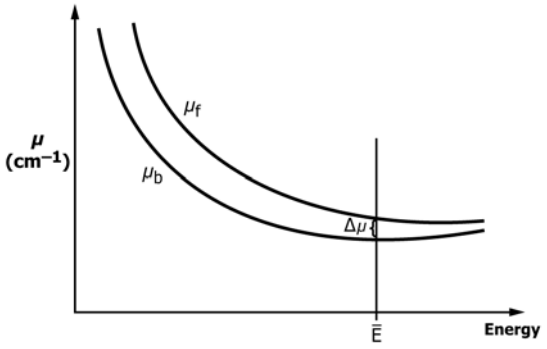

FIG. 12 A Sketch Illustrating the Dependence of Contrast Difference Δμ Upon the Energy of Incident X-Rays

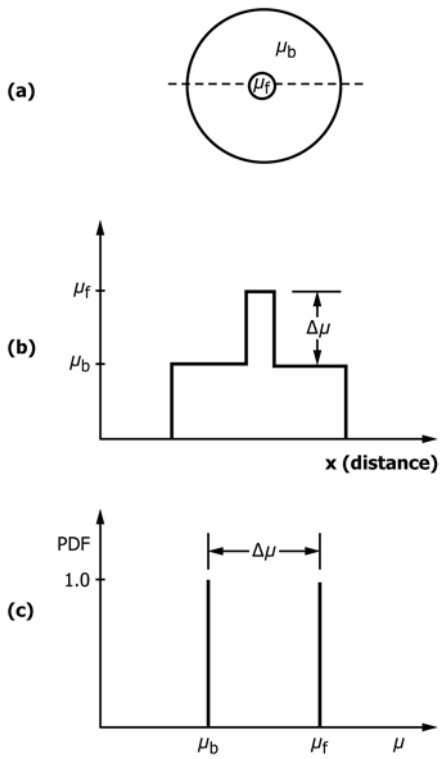

FIG. 13 (a) A Sketch Illustrating a CT Reconstruction of a Small Feature of Attenuation Coefficient μ_f Embedded in the Center of a Background Material of Attenuation Coefficient μ_b; (b) A Plot of the CT Density Profile Through the Feature in (a); and (c) A Probability-Distribution Function (PDF) for the Attenuation Coefficients Found in (a)

As resolution and noise are introduced into the discussion, the effect of each on the profile of Fig. 13(b) and the PDF of Fig. 13(c) will be monitored.

8.3 *Resolution*—The finite number and width of the X-ray beams causes the blurring of a feature, which can alter both the shape of the feature and the resolvability of multiple features. This blurring also affects the perceived contrast, especially of small features. To a first approximation, it is possible to derive a two-dimensional blurring function that can be convolved with an object to produce the equivalent of a CT image. This blurring function, called the point-spread function (PSF), is the response of the system to an ideal point object. In this discussion, it will be assumed that the PSF has circular symmetry and is uniform throughout the image. In this case, the modulus of the one-dimensional Fourier transform of a profile through the PSF gives the modulation-transfer function (MTF) (**71**) of the system, which describes the differential ability of the system to reproduce spatial frequencies. In general, low frequencies (large, homogeneous features) are reproduced more faithfully than high frequencies (small features).

8.3.1 First, a simple approximation to the PSF is discussed, and its effect on the profile of Fig. 13(b), on the PDF of Fig. 13(c), and on the effective contrast of small features is illustrated. Three methods of obtaining the MTF are then discussed: one theoretical and two experimental. It should be emphasized that the MTF is not merely a computational curiosity; it is used both to predict and to measure system performance.

8.3.2 For the purpose of illustration, the PSF can be approximated by a cylinder of diameter *BW* (**72**) that approximates the beam width. *BW* is a function of the detector width *d*, the X-ray source width *a*, the distance between the source and the detector *L*, and the distance between the source and the imaging point *q* as follows:

$$BW \simeq \frac{\sqrt{d^2 + [a(M-1)]^2}}{M} \tag{10}$$

where:

$$M = \frac{L}{q} \tag{11}$$

The quantities *d*, *a*, *L*, and *q* are illustrated in Fig. 14. A justification for Eq 10 will be given in the discussion of the MTF that follows (see also Ref (**72**)).

8.3.3 Fig. 15 shows the convolution of the PSF with features that are smaller than, equal to, and greater than the PSF. Fig. 15(a) shows the result of convolving the PSF of diameter *BW* with a smaller feature of diameter *SW* and contrast difference Δμ. The imaged feature will be a truncated cone with base (*BW* + *SW*) and contrast difference Δμ(*SW*/*BW*).^{2} Thus, the system PSF reduces the contrast of features smaller than the beam width by the ratio of their areas and increases the width of the imaged feature to approximately that of the PSF. Fig. 15(b) shows the result of convolving the PSF of diameter *BW* with a feature of diameter *BW* and contrast Δμ. The imaged feature will be a cone of base 2*BW* and maximum contrast difference Δμ. Fig. 15(c) shows the result of convolving the

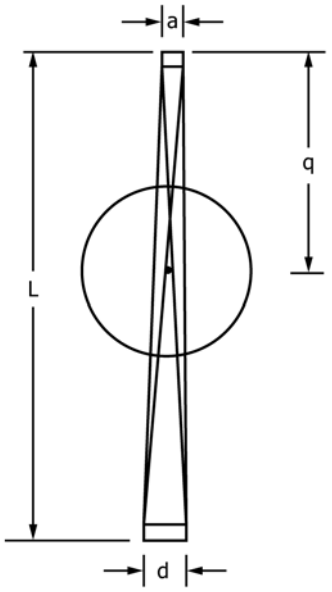

FIG. 14 A Sketch Illustrating the Geometry of the X-Ray Beam of a CT Scanner, Where *d* is the Detector Width, *a* is the X-Ray Source Width, *L* is the Distance Between the Source and the Detector, and *q* is the Distance Between the Source and the Imaging Point

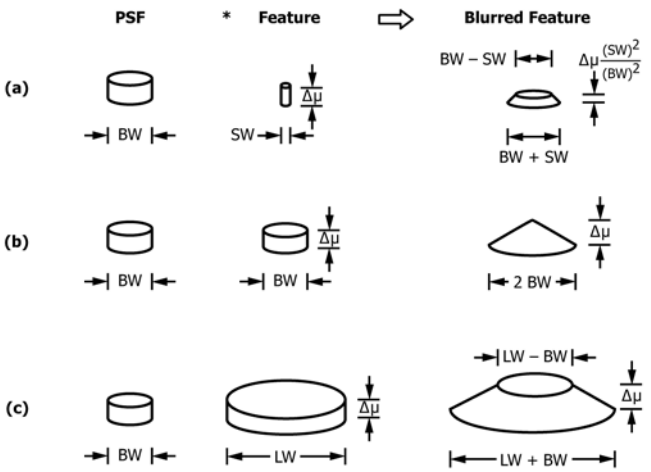

FIG. 15 A Sketch Illustrating the Two-Dimensional Convolution of a Point-Spread Function (PSF) of Diameter *BW* with Features of Varying Diameters: (a) *SW* < *BW*, (b) *BW* = *BW*, and (c) *LW* > *BW*. The Symbol (*) Represents the Convolution of Two Functions

PSF of diameter *BW* with a larger feature of diameter *LW* and contrast difference Δμ. The imaged feature will be a truncated cone of base (*BW* + *LW*) and contrast difference Δμ. Thus, the diameters of features much wider than the PSF are affected only slightly, and the contrast in their centers is not altered. These results will prove very useful later in the discussion on the relationship between detectability and feature size.

8.3.4 The fact that the CT imaging process is discrete rather than continuous has been ignored thus far. In fact, the projection data is sampled at some discrete spatial increment, *s*. Sampling theory dictates that *s* be *BW*/2 at most. The presentation of the reconstructed image is also discrete. Again,

sampling theory holds that pixel size, Δp, in the reconstructed image should be equal to or smaller than s to preserve spatial resolution. In terms of the convolution of Fig. 15, the smallest feature will occupy at least four (2^2) pixels, and possibly more.

8.3.5 Fig. 16(a) shows the effects on image fidelity that convolution with the PSF and discrete sampling has had on the ideal image of Fig. 12(a). The profile through the feature is now rounded at the edges. Fig. 16(b), which is a plot of the new probability-distribution functions (PDFs), shows that the PDF of the background now has values larger than μ_b and that the PDF of the feature has values smaller than μ_f.

8.3.6 The convolution of multiple features in the image with the PSF of the system illustrates the concept of the modulation-transfer function (MTF). Fig. 17 shows a central, one-dimensional profile of the convolution of the PSF of width *BW* with periodic features of diameter *D* whose centers are separated by 2*D*. These periodic features are dominated by spatial frequencies of value 1/(2*D*). Notice that as long as $D \geq BW$, the effective contrast $(\Delta\mu)_e$ is not reduced; whereas for $D < BW$, the effective contrast is reduced. Furthermore, there is no contrast at all at approximately $D = BW/2$. This spatial frequency at approximately 1/*BW* is called the cut-off frequency and represents the effective resolution limit of the system because frequencies above this value are significantly altered by the system and cannot contribute to a faithful representation of the object. Fig. 18(d) shows a plot of the ratio of the effective contrast, $(\Delta\mu)_e$, to the true contrast, $\Delta\mu$, as a function of the spatial frequency 1/(2*D*). This is the MTF curve. It can be measured experimentally for a real system from scans of spatial gauges similar to those of Fig. 17.

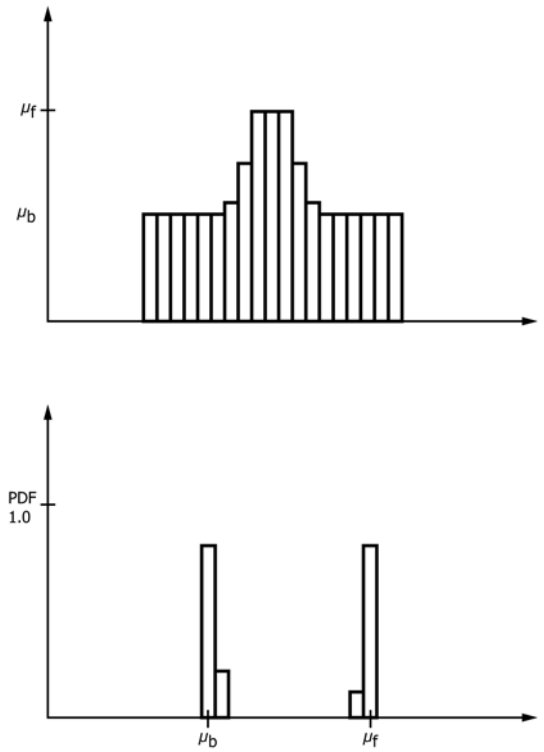

FIG. 16 (a) A One-Dimensional Profile Through the Center of a Feature Convolved with a CT PSF and Pixelized; and (b) A Probability-Distribution Function for the Profile in (a)

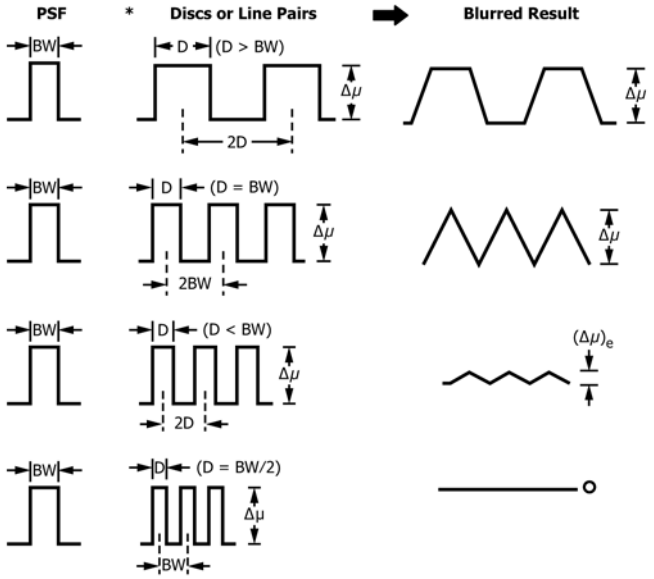

FIG. 17 An Illustration of a One-Dimensional Profile Through the Center of Periodic Features of Varying Diameters Which Have Been Convolved With a CT PSF: (a) *D > BW,* (b) *D = BW* , (c) *BW*/2 < *D* < *BW*, and (d) *D = BW*/2

However, this method is open to interpretation and is not recommended for an impartial system analysis.

8.3.7 The following discussion describes how to obtain a theoretical expression for the MTF of a hypothetical system. The formalium applies to a parallel-beam method of data collection, but the expressions for fan-beam data collection are analogous. The method is attributed to Glover and Eisner (**71**), who show that the MTF is approximately equal to the one-dimensional Fourier transform (FT) of a circularly symmetric PSF and is given by the following expression:

$$MTF(f) = \frac{F_{CON}(f)}{f} F_{BW}(f) F_{MOV}(f) F_{INT}(f) F_{PIX}(f) \qquad (12)$$

where:

$F_{CON}(f)$ = the FT of the convolution function,
$F_{BW}(f)$ = the FT of the effective beam width,
$F_{MOV}(f)$ = the FT of the data integration factor,
$F_{INT}(f)$ = the FT of the linear interpolation function in the image reconstruction,
$F_{PIX}(f)$ = the FT of the display function, and
f = the spatial frequency variable. Each of these factors will be described briefly.

8.3.8 The factor $F_{CON}(f)/f$ is the convolution filter factor, assuming a reconstruction process of parallel-beam convolution and backprojection. (The reconstruction process is beyond the scope of the present discussion.) The interested reader is referred to Ramachandran (**73**) or Shepp and Logan (**74**). The filter factor due to Ramachandran is used when high resolution is desired and the contrast is large enough that noise is not an issue. The filter factor due to Shepp and Logan is used when noise is high, contrast is low, and high resolution is not the primary objective. The factors for these two filters are given below, where s is the linear spacing between samples in a profile:

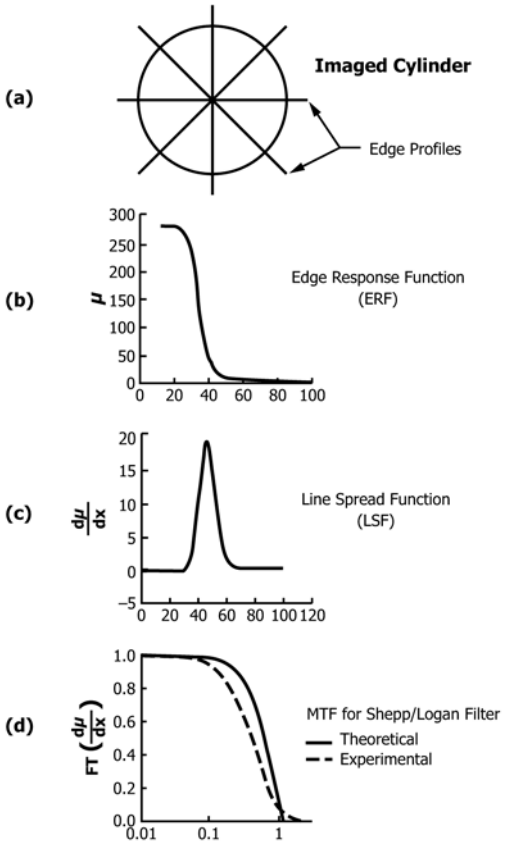

FIG. 18 An Illustration of the Procedure for Obtaining the MTF From a CT Image of a Small Cylinder: (a) Sketch indicating Relative Orientation of Three Different Line Profiles Through the Center of the Imaged Cylinder; (b) The Result of Aligning and Averaging Many Edge Profiles, the Edge-Response Function, ERF; (c) The System Line-Spread Function, LSF, Obtained by Differentiation of the ERF; and (d) The System Modulation-Transfer Function, MTF, Obtained by Discrete Fourier Transformation of the LSF

$$\frac{F^{R}_{\mathrm{CON}}(f)}{f} = 1 \ [\text{Ramachandran}] \tag{13}$$

$$\frac{F^{S\&L}_{CON}(f)}{f} = \frac{\sin(\pi fs)}{\pi fs} \ [\text{Shepp and Logan}] \tag{14}$$

8.3.9 Yester and Barnes (**72**) describe the FT of an arbitrary beam shape as follows, where these quantities are defined in Eq 10 and Eq 11:

$$F_{\mathrm{BW}}(F) = \frac{\sin\left[\frac{\pi fd}{M}\right]}{\frac{\pi fd}{M}} \frac{\sin\left[\frac{\pi fa(M-1)}{M}\right]}{\frac{\pi fa(M-1)}{M}} \tag{15}$$

They also note that this function can be approximated to a good approximation by the FT of a square beam whose width is *BW*, given previously by Eq 10.

8.3.10 Collecting discrete signals from a moving X-ray source is equivalent to convolution by a square function whose width is the linear sampling increment *s*. Its FT is given by the following:

$$F_{\mathrm{MOV}}(f) = \frac{\sin(\pi fs)}{\pi fs} \tag{16}$$

8.3.11 Since data values are computed at discrete points and the reconstruction process requires values at intermediate points, some form of interpolation must be conducted. One common form is linear interpolation whose FT has the following form:

$$F_{\mathrm{INT}}(f) = \frac{\sin^2(\pi fs)}{(\pi fs)^2} \tag{17}$$

8.3.12 Finally, the interpolated data are displayed on a square grid of width Δp. Since this representation is equivalent to a convolution, the MTF is also multiplied by the following factor:

$$F_{\mathrm{PIX}}(f) = \frac{\sin(\pi f \Delta p)}{\pi f \Delta p} \tag{18}$$

8.3.13 Eq 12 is useful for predicting the MTF of a hypothetical system. The relationship between the PSF and the MTF also suggests a superior method for measuring the MTF of an existing system. Since the PSF is ideally the system response to a point function, a point can be imaged, and the PSF can be obtained directly as a profile of this point image. In practice however, point objects always have some width. Fortunately, it can be shown that the one-dimensional profile of a circularly symmetric PSF is roughly equivalent to a profile taken perpendicular to the two-dimensional response of the system to a line, the line-spread function (LSF) (**75**). Although a line is equally difficult to image, the LSF is well approximated by the first derivative of the response of the system to an edge, the so-called edge-response function (ERF), which is obtained easily.

8.3.14 Fig. 18 illustrates the process of obtaining the MTF experimentally from the image of a simple cylinder. The use of a cylinder (Fig. 18(a)) is preferred because, once its center of mass is determined, profiles through this point are perpendicular to the cylinder edge. Many profiles can be aligned and averaged to reduce system and quantization noise on the edge-response function (ERF) (Fig. 18(b)). The LSF is estimated by taking the discrete derivative of the ERF (Fig. 18(c)), and its discrete FT is taken to obtain the MTF (Fig. 18(d)). (Note that, by convention, the height of the MTF is normalized to unity.) This procedure is easy to execute and not open to misinterpretation.

8.4 *Noise*—In the previous section, the extent to which the system PSF degrades contrast and resolution has been investigated. However, no factor has been introduced thus far that would prevent detection of a feature (except at the cutoff frequency). In this section, system noise is added to the model of system behavior, and its impact on detectability is explored in terms of basic system performance parameters.

8.4.1 It is not possible to build an X-ray CT imager without noise. Even if electronic noise and scatter noise are minimized, quantum statistics dictates that there will be variation in the number of X-rays detected from the source. The photon noise on the X-ray signal is known to obey Poisson statistics; that is, it is characterized by the fact that the variance of the signal is equal to its mean. It is customary to specify noise as the standard deviation, which is the square root of the variance. This means that if an average of *n* photons is detected in a given sampling period, the number actually recorded in any

particular interval will be in the range of $n \pm \sqrt{n}$ approximately 70 % of the time.

8.4.2 The effect that noise has on a CT image is complicated by the reconstruction process. For a parallel-beam scanner geometry, Barrett and Swindell (**76**) show that the noise at the center of a reconstructed cylinder of radius R_o irradiated by X-rays of effective energy $\bar{E}$ is given by the following formulas for the Ramachandran (σ_R) and Shepp and Logan ($\sigma_{S\&L}$) convolution filters:

$$\sigma_R \simeq \frac{0.91}{s\sqrt{V}}\sigma_d \text{ [Ramachandaran]} \tag{19}$$

$$\sigma_{S\&L} \simeq \frac{0.71}{s\sqrt{V}}\sigma_d \text{[Shepp and Logan]} \tag{20}$$

where:

V = the number of views or orientations,
s = the spatial sampling increment, and
σ_d = the standard deviation of the noise on the samples in the profile data.

The computation of the noise on the profile data, σ_d, is complicated by the fact that the profile data is the natural logarithm of the ratio of the intensity of the unattenuated radiation, n, and the detected signal. Also, there is likely to be additional noise from the detector electronics and scattered radiation. In a detailed analysis, these contributions must be included, and they will increase the noise. However, in the approximation that photon noise dominates, the minimum possible data noise, σ_d, is given by the following expression, where $\mu_o(\bar{E})$ is the linear attenuation coefficient of the cylinder:

$$\sigma_d \simeq \left[\frac{1}{n\exp\left[-2\mu_o(\bar{E})R_o\right]} + \frac{1}{n}\right]^{1/2} \tag{21}$$

Notice that the noise decreases with increasing n and increases with increasing R_o or μ_o.

8.4.3 Experimentally, the usual process for determining the standard deviation, σ, for a homogeneous area of a reconstructed image containing m pixels, each with some value μ_i, is to first find the mean value of the set of m pixels:

$$\bar{\mu} = \frac{1}{m}\sum_{i=1}^{m}\mu_i \tag{22}$$

and then compute σ as:

$$\sigma = \left[\frac{\sum_{i=1}^{m}(\mu_i - \bar{\mu})^2}{m-1}\right]^{1/2} \tag{23}$$

where:

Σ = summation over the region of interest, and
σ = a measure of the spread of the values of μ_i about the mean $\bar{\mu}$.

Hanson (**77**) shows that σ is not very sensitive to the number of pixels averaged if m is in the range of $25 \le m \le 100$. The noise in a reconstructed image does have a positional dependence, especially near the edges of an object, so extremely large regions should not be used. Hanson (**78**) has also shown that the noise in CT images is not completely uncorrelated, but the effect on σ is small.

8.4.4 Fig. 19(a) shows the effect that noise has on the blurred, pixelized image of Fig. 16(a). The noise appears as a jitter superimposed on the profile of the feature. Fig. 19(b), which shows the new PDFs, illustrates that the spread of attenuation values has increased and that the two distributions may overlap. The photon noise on any one sample is Poisson distributed, but the combination of independent samples is approximated better by the normal distribution given by the following expression:

$$\text{PDF}(\mu) = \frac{1}{\sqrt{2\pi}\sigma}\exp\left[-\frac{(\mu-\bar{\mu})^2}{2\sigma^2}\right] \tag{24}$$

where:

$\bar{\mu}$ = the mean of the distribution, and
σ = the standard deviation.

Eq 24 has the advantage of being computationally simple. Fig. 19(c) shows the PDFs redrawn as smooth curves. The figure illustrates the fact that 70 % of the values are within $\pm\sigma$ of the mean.

8.4.5 Fig. 19(c) shows that the contrast will be degraded. The difference in contrast can now be defined to be the difference between the mean of the feature, $\bar{\mu}_f$, and the mean of the background, $\bar{\mu}_b$. However, if a detection threshold is placed between the two distributions and they overlap, there will be instances when pixels within the feature will be counted as features.

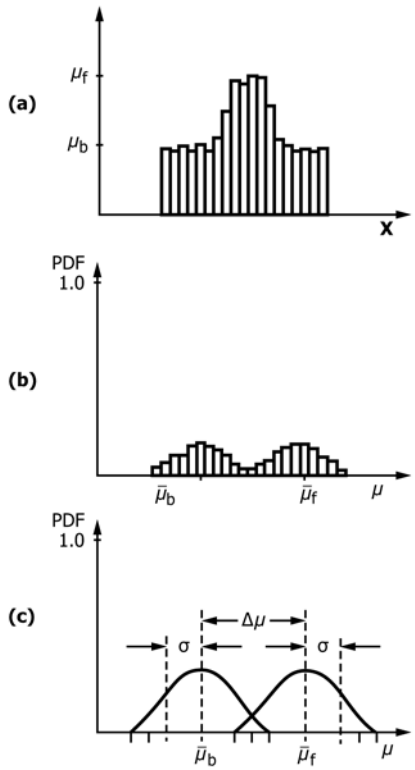

FIG. 19 (a) A Line Profile Through the Center of a Noisy Feature Convolved With a CT PSF and Pixelized: (b) A Probability-Distribution Function for the Profile in (a); and (c) A Continuous Representation of the PDFs of (b) With the Means, Standard Deviations, and Contrast Difference Indicated

8.5 *Contrast-Detail-Dose (CDD) Curve*—In practice, detection is not based solely on threshold criteria. Human beings use visual integration when detecting features, and even computer detection processes are likely to use pattern recognition techniques. Thus, detection criteria should be based on the observations of human beings. Several investigators (**77, 79, 80**) have reported that the effective contrast, $(\Delta\mu)_e$, which human beings can detect with a 50 % probability of success, depends on the image noise, σ, and the object diameter, *D*, according to the following relationship:

$$(\Delta\mu)_e \simeq \frac{c\sigma\Delta p}{D} \tag{25}$$

where:

Δp = the pixel width, and
c = a constant in the range of $2 \le c \le 5$.

8.5.1 It is seen from Fig. 15 that the contrast difference of features larger than the effective beam width *BW* is not affected by beam convolution. Thus, for large features:

$$(\Delta\mu)_e = \Delta\mu \simeq \frac{c\sigma\Delta p}{D} \; [D >> BW] \tag{26}$$

Dividing Eq 26 by μ_b and multiplying by 100 % gives the formula for percent contrast:

$$\frac{|\mu_f - \mu_b|}{\mu_b}\,100\,\% = \frac{c\sigma\Delta p}{D\mu_b}\,100\,\% \; [D >> BW] \tag{27}$$

8.5.2 Eq 25 has not been tested for features smaller than *BW*. However, the results of Fig. 15 suggest a logical extension. Features smaller than *BW* have effective diameter *BW* and have the contrast reduced by $D^2/(BW)^2$. Thus, the detectability limit for smaller features can be approximated by the following:

$$(\Delta\mu)_e = \frac{\Delta\mu D^2}{(BW)^2} \simeq \frac{c\sigma\Delta p}{BW} \; [D << BW] \tag{28}$$

and the percent contrast is given by the following:

$$\frac{|\mu_f - \mu_b|}{\mu_b}\,100\,\% \simeq \frac{c\sigma BW\Delta p}{D^2\mu_b}\,100\,\% \; [D << BW] \tag{29}$$

8.5.3 Detectability alone is often not sufficient; features must be discriminated (detected and resolved). Eq 25 can also be used to predict the discrimination of pairs of features of diameter *D* separated by 2*D*. (This distance is used because it is conventional to define resolvability in terms of the classical Rayleigh sense, which stipulates a 2*D* separation.) From Fig. 17, it has been shown that in this case, $(\Delta\mu)_e$ is given by the product of the true contrast times the system modulation-transfer function (MTF). In this case, the perceived contrast, $(\Delta\mu)_e$, is given by the following expression:

$$(\Delta\mu_{CDD})_e = \Delta\mu_{CDD} \times MTF\left(\frac{1}{2}D\right) = \frac{c\sigma\Delta p}{D} \tag{30}$$

Solving Eq 30 for $\Delta\mu_{CDD}$, dividing by μ_b, and multiplying by 100 % gives an expression for the percent contrast for threshold (50 %) discrimination:

$$\frac{|\mu_f - \mu_b|}{\mu_b}\,100\,\% = \frac{c\sigma\Delta p \times 100\,\%}{\mathrm{MTF}\left(\frac{1}{2}D\right)D\mu_b} \; [\mathrm{CDD}] \tag{31}$$

The plot of the contrast required for 50 % discrimination of pairs of features as a function of their diameters in pixels is called a contrast-detail-dose (CDD) curve.

8.6 *Performance Prediction*—The detectability limits defined by Eq 27 and Eq 29 can be used to estimate the detection ability of a proposed CT system to detect an object of a given size and composition. In the interest of simplicity, detectability will be computed at the center of a uniform cylinder. The noise in a reconstructed cylinder is highest at its center so that this represents a worst case. Also, many complex objects can be approximated by a cylinder of the same material and cross-sectional area.

8.6.1 The contrast given in Eq 27 and Eq 29 is a function of μ_b, which in turn depends on the X-ray source effective energy $\bar{E}$, the pixel size Δp, the size of the feature relative to the X-ray beam width *BW*, and the noise σ. Many references list linear attenuation coefficients as functions of $\bar{E}$ (**81, 82**). *BW* is defined by Eq 10 and Fig. 14 in terms of the source width, detector width, and position of the object. For a parallel-beam CT scanner, σ is given by Eq 19 and Eq 20 in terms of the sampling increment *s*, the number of views *V*, the cylinder radius R_o, and the number of unattenuated photons incident in each sample *n*. Once these parameters are specified, it is possible to plot a detectability graph that will predict the performance of the scanner.

8.6.2 Fig. 20 shows the detectability graph for an iron cylinder 2.54 cm in radius that is irradiated with 0.8 MeV X-rays. The detectability line for objects of diameter $D >> BW$ (Eq 27) is represented by a solid line. For ease of analysis, the $\log_{10}$ of the percent contrast has been plotted as a function of the $\log_{10}$ of the feature diameter, *D*, measured in pixels. The detectability line for objects of diameter $D << BW$ (Eq 29) is represented by a dashed line. To determine whether a feature of given diameter, *D*, and linear attenuation, μ_f (0.8 MeV), will be detected in the center of this iron cylinder, plot the point whose ordinate is the percent contrast, 100 % × $|\mu_{FE}$ (0.8 MeV) – μ_f

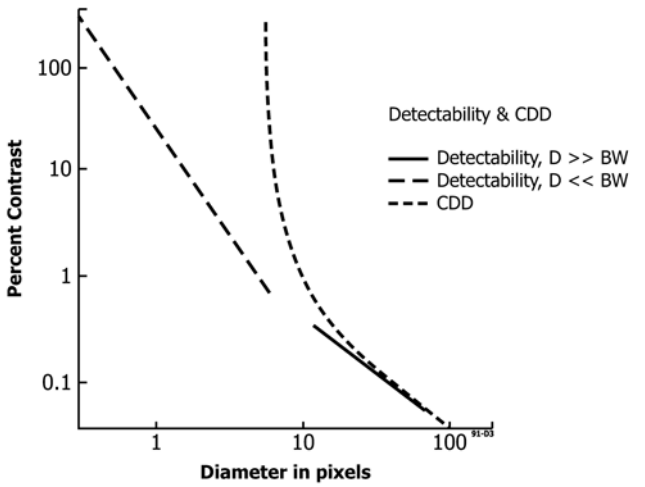

FIG. 20 A Plot Illustrating the Application of the Detectability Lines and the CDD Curve for a Cylinder of Iron of Radius 2.54 cm that is Irradiated By 0.8-MeV X-Ray Photons: A Value of 8.5 was used for the Constant *c* in Eq 25 and its Derivative Equations

(0.8 MeV)l/μ_{FE} (0.8 MeV) and whose abscissa is the diameter *D* in pixels. If this point falls well to the right of the lines, it will be detected more than 50 % of the time. If it falls to the left, it will not. Remember that the percent contrast must be multiplied by the ratio *h/t* if the height of the feature *h* is less than the X-ray slice width *t*.

8.6.3 It is also possible to plot the theoretical CDD curve specified by Eq 31. The theoretical MTF has been given in Eq 12 as a function of specified scanner parameters. The theoretical CDD curve for the iron cylinder is identified in Fig. 20 by the short dashed curve. To determine whether two features of diameter *D* whose centers are separated by 2*D* can be discriminated at least 50 % of the time, plot a point whose ordinate is the percent contrast and whose abscissa is their common diameter in pixels. Determine the position of the point relative to the curve. If it lies well to the right of the curve, the features will be discriminated with at least a 50 % probability.

8.7 *Performance Verification*—The detectability and CDD curves for an existing CT scanner can also be plotted from Eq 27, Eq 29, and Eq 31 for a cylinder of specified material and size. The quantity σ/μ_b is the noise-to-signal ratio at the center of the cylinder as computed from Eq 22 and Eq 23. The function MTF(½ *D*) is computed experimentally from a small cylinder as described in Fig. 18. Fig. 21 shows a comparison of the predicted (solid line) and measured (dotted line) CDD curves from an existing CT scanner for an iron cylinder 2.54 cm in radius irradiated by an equivalent energy of 0.8 MeV. A comparison between the experimental and theoretical MTF curves is shown in Fig. 18d. The agreement between the theory and experiment is quite good in this case. Because the cylinder is relatively small, there is not a large contribution to the noise from scattered radiation. For a large cylinder, scatter will usually make the experimental noise larger than the predicted noise, and the curve will shift upwards.

8.8 *Conclusion*—A simple formalism for the prediction and evaluation of the performance of X-ray CT systems has been presented. Contrast has been defined and the degradation of contrast by the system point-spread function and the system noise has been discussed. Finally, the use of a simple object has been recommended to predict and verify the performance of CT systems in the detection and discrimination of features in a background of specified size and composition. It must be emphasized that this formalism is meant to be a simple indicator of system capabilities and does not address such complications as detection in the presence of CT artifacts.

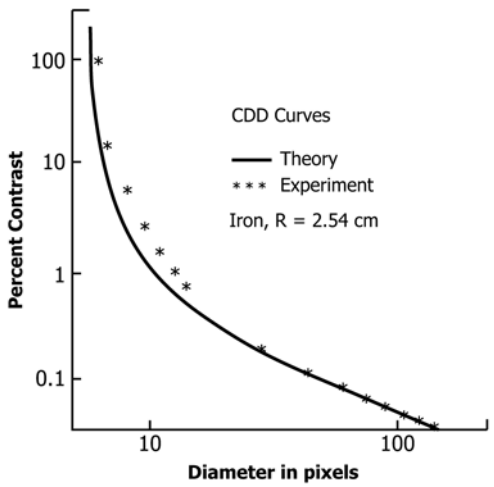

FIG. 21 A Comparison Between Predicted and Measured CDD Curves for a Real Scanner; The Object Scanned is an Iron Cylinder of Radius 2.54 cm that is Irradiated By 0.8-MeV X-ray Photons; A Value of 8.5 was used for the Constant *c* in Eq 25 and its Derivative Equations

9. Guidance for Precision and Bias

9.1 Computed tomography (CT) images are well suited for use in making quantitative measurements. The magnitude and nature of the error in CT-based measurements depends very strongly on the particulars of the scanner apparatus, the scan parameters, the object, and the features of interest. Among the parameters which can be estimated from CT images are feature size and shape, feature density contrast, wall thickness, coating thickness, absolute material density, and average atomic number.

9.2 The use of such quantitative measurements requires that the errors associated with them be known.

NOTE 1—This discussion addresses only the precision and bias of the *measurements*, not the noise or artifact in the images themselves.

9.3 The *precision* of the measurements can best be measured by seeing the distribution of measurements of the same feature under repeated scans, preferably with as much displacement of the object between scans as is expected in practice. This ensures that all effects which vary the result are allowed for; such as photon statistics, detector drift, alignment artifacts, spatial variation of point-spread-function, object placement, and so forth.

9.4 One source of such variation in measurements is uncorrected systematic effects such as gain changes or offset displacements between different images. Such image differences can often be removed from the measurement computation by including calibration materials in the image, which is then transformed so that the calibration materials are at standard values. Since air is usually already present in the image, a single additional calibration material (preferably similar to the object material, and placed in a standard position in the image) is often sufficient.

9.5 In addition to random variation, measurements of any particular feature may also have a consistent *bias.* This may be due to artifacts in the image or to false assumptions used in the measurement algorithm. When determined by measurement of test objects, such biases can be removed by allowing for them in the algorithm.

9.6 Examination of the distribution of measurement results from repeated scans of test objects with known features similar to those which are the target of the NDE investigation is the best method of determining precision and bias in CT measurements. Once such determinations have been made for a given system and set of objects and scanning conditions; however, they can be used to give well-based estimates of precision and

bias for objects intermediate in size, composition and form, as long as no unusual artifact patterns are introduced into the images.

10. Keywords

10.1 computed tomography (CT); contrast; contrast-detail-dose (CDD); detectability; imaging; modulation transfer function (MTF); nondestructive evaluation (NDE); pointspread function (PSF); reconstruction; resolution; scan; X-ray attenuation

APPENDIX

(Nonmandatory Information)

X1. GLOSSARY

X1.1.1 **afterglow**—Afterglow varies substantially between different types of scintillator, and is negligible in many CT measurement situations.

Discussion—Afterglow varies substantially between different types of scintillator, and is negligible in many CT measurement situations.

X1.1.2 **air measurement**—a reference radiation-intensity measurement made with no object in the examination region of a tomograph.

Discussion—Air measurements are used with radiation-intensity measurements through an object to infer opacity. An air measurement is required for each detection element. If the radiation source moves relative to the detection elements, a set of air measurements will generally be required for each source position.

X1.1.3 **analytical reconstruction techniques**—methods for computing a map of internal CT density from opacity measurements, based on mathematical integration techniques for directly inverting the Radon transform, which the process of measurement approximates.

Discussion—Contrasted to iterative reconstruction techniques. Analytical techniques using Fourier transforms are the basis of almost all commercial CT reconstructions.

X1.1.4 **aperture function, detector**—a three-dimensional function centered on the axis from the radiation source to a detector element, giving the sensitivity of the detector to the presence of attenuating material at each position.

Discussion—The detector aperture function gives the extent and intensity distribution of each ray around and along the length of its central line. The function is determined by the size and shape of the radiation source and of the active region of the detector, and by relative distance to the source and the detector. The average width of this function in the region of the object being examined is an important limit on the spatial resolution of a CT scan.

X1.1.5 **area detector**—an X-ray detection apparatus with numerous individual elements arranged in a pattern spread over two dimensions, such as a fluoroscopic screen.

Discussion —This is in contrast to a linear detector array such as used in many tomographic systems

X1.1.6 **artifact, CT**—a discrepancy between the actual value of some physical property of an object and the map of that property generated by a CT imaging process.

Discussion—The term artifact is usually restricted to repeatable discrepancies, with other variations classed as noise. The most common tomographic artifacts result from undersampling the object (where there is object detail finer than the measurement spacing), uncorrected physical effects (such as cupping from beam hardening), and incorrect calibration of detector response or apparatus position.

X1.1.7 **attenuation coefficient, X-ray**—a measure of the rate at which the material in a particular region attenuates an X-ray beam with a particular spectrum as it passes through.

Discussion—Of particular relevance to CT is the linear attenuation coefficient, which is the decrease in radiation intensity per unit of distance traveled, for a particular substance and radiation-beam composition. Units for this coefficient are typically cm^{-1}. The linear attenuation coefficient is the mass attenuation coefficient multiplied by the mass density of the substance. The CT density in each pixel of a tomogram is basically a linear-attenuation-coefficient value (perhaps with a scaling factor), although artifacts may cause local or global deviations. This coefficient is the sum of the coefficients for several physical attenuation processes (scattering, photoelectric absorption, and/or pair production), each of which varies substantially with the X-ray photon energy and the elemental composition of the material. The integral of the linear attenuation coefficients along a ray path gives the X-ray opacity for that ray in the dimensionless natural units called attenuation lengths.

X1.1.8 **attenuation length**—the dimensionless natural unit of X-ray projection values along rays through an object, in terms of the natural logarithm of intensity reduction.

Discussion —An opacity of n attenuation lengths implies that the fraction of a photon beam passing through the object without interaction is $1/e^n$. (For multienergetic beams, each energy group is weighted by the signal it generates.)

X1.1.9 **attenuation, X-ray**—the process of reduction of radiation-beam intensity due to interactions during passage through matter.

Discussion—Each of the penetrating photons emitted from an X-ray source has a probability of interaction with material in its path, dependent on the photon energy and on the thickness, density, and elemental composition of the material.

Almost all of these interactions will result in the photon being absorbed or scattered so that it will not reach the detector toward which it was originally travelling. The photons remaining in the primary beam are not reduced in energy or changed in any way; thus X-ray beam attenuation is an all-or-nothing process for the individual photons, unlike the gradual loss of energy by each particle in charged particle beams.

X1.1.10 **backprojection**—the process of adding to each pixel a contribution from a (possibly interpolated) value associated with a line through it, as part of the process of reconstruction of a CT-density map of an object from measurements through it.

Discussion—The values to be backprojected are derived from groups of measurements, which are usually organized in views, each of which is a projection of the object from one direction. For other than parallel-beam views, a weighting factor (based on distance from the radiation source for fan-beam views) is also used.

X1.1.11 **beam hardening**—the shift in the proportions of the energies in a multienergetic beam of penetrating radiation resulting from the preferential attenuation of the less-penetrating photons.

Discussion—The beam photons which pass through an object without interaction are, on the average, more penetrating or "harder" than the original set which entered the object. (Since the penetrating power of X-rays generally increases with energy, hardening usually increases the average energy of the beam.) Failure to correct for the non-linearity in opacity caused by this change in beam composition may cause characteristic "cupping" or "diagonal" artifacts in tomograms. Spectral shifts of this kind can be substantially reduced by suitable beam filtration to remove the least-penetrating portions of the beam.

X1.1.12 **beam width**—the distance normal to the axis of a ray of penetrating radiation over which changes in object opacity will substantially influence the signal generated.

Discussion —Typically an average value based on the aperture function in the region of the object is taken to characterize this parameter. The beam width may differ in different directions due to the shape of the source spot or detector aperture. For fan beams, the beam width in the direction normal to the plane of the fan is called the slice thickness.

X1.1.13 **CAT**—Computed Axial Tomography, an earlier term for what is now known as computed tomography (CT).

Discussion—The term "axial" was used to distinguish the method from focal-plane tomography.

X1.1.14 **collimation**—the restriction of the possible paths for radiation by placement of absorbing material.

Discussion—Collimation near the radiation source is used to limit the radiation beam to correspond to the general shape of the detection apparatus. In some cases, further collimation near the detector bank or for each detector is used to reduce or eliminate scattered radiation from that which will ultimately be measured.

X1.1.15 **Compton scattering**—a type of interaction between a photon and an electron, in which part of the photon's energy is transferred to the electron as kinetic energy.

Discussion —The probability of this type of interaction is proportional to the local electron density. For the range of photon energies and objects used in normal CT scans, it decreases gradually with increasing photon energy, and is generally the most likely mode of attenuation in light materials or at intermediate (0.1 to 10 MeV) photon energies. Also called inelastic scattering.

X1.1.16 **computed tomography (CT)**—a nondestructive examination technique in which penetrating-radiation measurements of the X-ray opacity of an object along many paths are used to compute a cross-sectional CT-density map called a tomogram.

Discussion—In the original approach, the measurements are planar views made up of overlapping measurements along rays from many regularly-spaced directions, all centered on a slice plane. Approaches using a cone beam have also been developed.

X1.1.17 **cone beam**—the diverging radiation from a source shaped by collimation into a pattern whose dimensions at any given distance from the source are roughly the same in all directions, typically directed at an area detector.

Discussion—This is in contrast to a fan beam or a pencil beam.

X1.1.18 **cone-beam CT**—use of cone-beam X-ray opacity measurements from many directions to estimate CT density throughout a three-dimensional volume of an object.

Discussion—Using two-dimensional area detectors, measurements may be made rapidly through all of an object at once. Such measurements from many directions can be used to compute CT-density values throughout the volume. The speed, efficiency, X-ray energy range, resolution, artifacts, noise, and scatter-rejection capabilities of systems utilizing such cone-beam methods can differ substantially from systems using fan-beam methods based on linear detector arrays.

X1.1.19 **contrast**—the extent to which a parameter of interest differs for some set of features.

Discussion—Thus the contrast in linear attenuation coefficient ("CT density") of aluminum (0.33 cm^{-1}) to iron (1.15 cm^{-1}) is – 0.82 cm^{-1}, for photons of 200 KeV. Contrast is often stated as the percentage by which the value for one feature is greater or less than the value of the other ("aluminum has a 71 % CT-density contrast to iron at 200 KeV"). Contrasts in the physical properties of different parts of an object may result in contrasts in the image densities for tomograms or radiograms. Since CT density varies with energy quite differently for different materials, the contrast in tomograms can be strongly influenced by beam energy, usually increasing with lower energy. Since image noise usually increases with lower energy even more, image contrast is an incomplete measure of the ease of distinguishing features; see density resolution and contrast-detail diagram.

X1.1.20 **contrast-detail diagram**—a diagram showing, for a given imaging situation, the contrast at which features of various sizes (and perhaps shapes) can be distinguished with some specified confidence.

Discussion—Such a CDD summarizes the impact of the

noise and blurring in an image on a decision process. Such a diagram is most dependable when it represents empirically-verified tests conducted under actual operating conditions (thus including operator performance and effects specific to a particular inspection task), but diagrams computed from measures of spatial and density resolution can also be useful.

X1.1.21 **contrast sensitivity**—see *density resolution*.

X1.1.22 **convolution**—the transformation of an ordered array of numbers (such as a tomographic view) such that, for each position, a new number is formed from the weighted sum of some of the original numbers, with the weighing factors based only on the amount of difference in position.

Discussion—The array of weighting factors is called a convolution kernel. In most cases the weights decrease with increasing distance; the typical tomographic-reconstruction kernel is $-1/d^2$ for nonzero distances d, with a positive weight at d = 0 large enough to make the sum of the weights zero. A process equivalent to convolution can be accomplished efficiently for large kernels with the Fast Fourier Transform (FFT) by multiplying each value of the transform of the data by the corresponding point of a frequency-space filter which is the transform of the kernel. An inverse FFT then converts this product array into the convolved data. The most common methods of tomographic image computation use the FFT to convolve each view of opacity measurements, and then back-project the resulting filtered line. The $-1/d^2$ kernel transforms into a filter proportional to frequency up to a cutoff frequency determined by the measurement spacing. The precise shape of the filter can be modified to minimize artifacts or to include any other linear filtering desired (see smoothing and sharpening).

X1.1.23 **crosstalk**—a condition in which activity in a measurement channel causes spurious activity in another (usually adjacent) channel.

Discussion—This may be due to scattering of radiation in the detector, or to optical or electromagnetic coupling of the signals resulting from detection. Software correction for known crosstalk patterns is often possible.

X1.1.24 **CT**—see *computed tomography*.

X1.1.25 **CT density**—the parameter, related to the action of each region of an object cross-section in attenuating an X-ray beam, which is computed for a two- or three-dimensional region by the computed tomography imaging process.

Discussion—(Note: the term "density" is used in several related but different senses (often without explicit distinction) in reference to CT: mass density, electron density, optical density, and image density, for example, as well as the CT density defined here.) For monoenergetic beams, CT density is proportional to the linear attenuation coefficient of each area of the object for the penetrating radiation used for the through-the-object X-ray measurements from which the image is computed. For multienergetic radiation, where the beam spectrum (and thus the attenuation coefficient) passing through each interior point varies with ray direction due to beam hardening, CT densities are averages. In some cases, such as objects made of a single known material, the CT-density measurements or images can be transformed to give values directly in mass density or some other physical parameter which is independent of the energy spectrum of the radiation used for measurement.

X1.1.26 **CT number**—a quantitative value for CT density, generally based on a linear scale between zero for air and a standard value for a reference material.

Discussion—CT-number values for a given object depend on the radiation spectrum as well as the object characteristics, especially for materials of different effective atomic number.

X1.1.27 **cupping**—an artifact in tomographic images, typically due to uncorrected beam hardening, in which the CT-density values in the interior of an object are reduced compared to those near the outside.

X1.1.28 **dark measurement**—a calibration measurement from each detection element made while the radiation source is closed or turned off.

Discussion—Dark measurements are used to correct each measurement with that detector. Also called offset measurement.

X1.1.29 **density**—amount per unit of volume (or, more rarely, of area or length); especially, the amount of mass per unit of volume (mass density), but the term is also used for analogous parameters such as electron density or CT density. A different use of the term is for the dimensionless parameters optical density and film density, measures of attenuation which are the logarithms of transmission ratios.

Discussion—Both usages are relevant in work with radiographic measurements, so adding the appropriate modifier when first using the term or when changing meaning is recommended to avoid confusion. Mass density is often the physical parameter of interest to the investigator in a CT examination; electron density can often be directly inferred from CT scans; CT density (closely related to the linear attenuation coefficient) is the parameter actually measured. In all these cases, a density map over two or three dimensions is used, approximated by values at discrete pixels or voxels. Optical (or film) density refers to a projection along a ray rather than a value at a single point; in fact, digital radiograms are computed density projections in this sense (based directly on the object's transmission of X-rays, not a film's transmission of light). These X-ray projection values which comprise a digital radiogram differ from film-density values in that high values mean less X-ray exposure (zero density is maximum exposure), and in the more dependable relationship between the projection values and the amount of attenuating matter, since exposure time is calibrated for and such sources of variation as film characteristics and development history are avoided.

X1.1.30 **density resolution, CT**—a measure of the extent to which a tomogram or radiogram can be used to detect differences in the physical parameter mapped by the image, for features of a given size.

Discussion—The limiting factor in CT density resolution is generally the noise in the image averaged over areas of the feature size; this may vary significantly between different regions of the image. Another important factor is the contrast that the features show under the scan conditions for this image. Taking the ratio of some multiple of the standard deviation of the image noise to a typical image density value is a common method for quantifying density resolution. Image artifacts may also limit resolution in certain cases. Note that the size of the

feature and all of the factors which influence image noise and contrast (beam energy, object size, scan time, etc.) must be specified for a comparison of density-resolution values to be meaningful.

X1.1.31 **detectability, CT**—the extent to which the presence of a feature can be reliably inferred from a tomographic inspection image.

Discussion—CT detectability is dependent on the spatial resolution and density resolution of the image, as well as the levels of confidence required that false positives and false negatives will be avoided. Features may be detectable even if they are too small to be resolved, provided their contrast after blurring is still sufficient.

X1.1.32 **detector**—a device which generates a signal corresponding to the amount of radiation incident on it.

Discussion—CT detectors are usually arranged in arrays in one or two dimensions.

X1.1.33 **detector spacing**—the distance (linear or angular) between adjacent radiation collection elements in a detector array.

Discussion—In most scanning systems this spacing determines one of the dimensions of the measurement spacing, although some systems use measurement interlacing to overcome this limitation if their detector spacing is large.

X1.1.34 **digital radiography (DR)**—formation of a map of projected X-ray opacity values through all or part of an object by digitization of signals derived from measurements of penetrating radiation.

Discussion—Such X-ray opacity maps can be produced by either a cone beam, used with an area detector such as a fluoroscopic screen or X-ray film, or by moving the object perpendicular to the plane of a fan beam directed at a linear detector array. Differences in scatter rejection, detection efficiency, and total detector active area give these approaches quite different characteristics. All DR techniques benefit from the great precision and flexibility in display and analysis that image-analysis software provides. Radiograms made by tomographic scanners are used both for direct object inspection and as "preview scans" to select the slice planes of interest for CT scans.

X1.1.35 **dimensioning accuracy**—the extent to which the actual dimensions of an object correspond to dimensions calculated from an image, such as a tomogram.

Discussion—For objects made of uniform-density materials with smooth surfaces, it is usually possible to obtain dimensions substantially more accurate than the spatial resolution of the image, especially if measurements can be averaged along a surface.

X1.1.36 **display matrix size**—the number of horizontal and vertical pixels available for display of images.

Discussion—Display matrix size has no direct connection with the spatial resolution of a tomographic system; however, insufficient display matrix size may require the use of image-zooming techniques to show images at full resolution.

X1.1.37 **DR**—see *digital radiography*.

X1.1.38 **dual-energy scanning**—use of two sets of measurements through an object taken with differing radiation-beam energy spectra to separate the effects of a mixture of materials.

Discussion—Because the variation with beam energy of the probability for each type of attenuation process is significantly different for most materials, it is possible to use two different-energy measurements along the same path in an object to solve for energy-independent physical parameters such as electron density and average atomic number. A common technique is to solve for the amounts of each of two predetermined basis materials whose mixture would give the pair of measurements seen. The separated energy-independent values derived from the measurements can be used to form separate maps (either tomograms or radiograms) of each basis material.

X1.1.39 **edge response function (ERF)**—the graph of CT density across an edge which shows how faithfully the image of a sharp edge is reproduced in a tomogram.

Discussion—The image of an edge proceeds in an "S-curve" from a background value through intermediate values (due to partial volume effects or reconstruction artifacts) to a limiting value (the interior CT density of the object). The width of the intermediate region is a good measure of the spatial resolution of an image. For images with little edge artifact, such as tomograms of low-opacity cylinders, the derivative of the edge response function is a good approximation to the line-spread function or point-spread function. The normalized Fourier transform of the point-spread function yields the modulation transfer function (MTF), which gives the relative frequency response of the imaging process.

X1.1.40 **elastic scattering**—an interaction between a photon and a bound electron in an atom, in which the photon is redirected with negligible loss of energy.

Discussion—The electron is not affected, with the recoil momentum being transferred to the atom as a whole. The effect is most pronounced at energies less than the binding energy of the electron, and its probability decreases with increasing energy. Also referred to as coherent scattering or Rayleigh scattering.

X1.1.41 **electron density**—the number of electrons per unit volume.

Discussion—The ratio of electron density to mass density is roughly constant, gradually decreasing from about 3.0×10^{23} electrons/gram for light elements (except hydrogen, which is twice this value) to 2.4×10^{23} for the heaviest ones. Because Compton scattering (the dominant attenuation process in many tomographic scans) is directly proportional to electron density, many tomograms are actually maps of electron density.

X1.1.42 **false negative**—an erroneous assertion of the nonexistence of a condition (such as a defect) by a decision process, often due to the limited resolution of a tomographic image.

Discussion—See *false positive*.

X1.1.43 **false positive**—an erroneous assertion of the existence of a condition (such as a defect) by a decision process, often due to noise or artifact when interpreting tomographic images.

Discussion—The incidence of false positives ("false alarms") depends on the decision criteria as well as the image;

decreasing the sensitivity of the process will generally decrease false positives, for example, but will increase false negatives. An analysis of the expected cost and incidence of each type of error is required to choose optimal decision criteria for any particular inspection process.

X1.1.44 **fan beam**—penetrating radiation from a small source, typically directed at a linear detector array, which has been shaped by collimation into a pattern which is wide in one direction and narrow in the orthogonal direction.

Discussion—In fan-beam CT systems, each measurement period gives a planar fan of measurements with a common vertex at the beam spot. Depending on the pattern of object motion, these measurements can be directly handled as fan-beam views or distributed into parallel-beam views. Contrasted to cone beam and pencil beam collimation.

X1.1.45 **field of view (FOV)**—the physical size of the area to be examined which must be subtended by the X-ray beam.

Discussion—If the test object is larger than the FOV or moves out of the FOV during scanning, unexpected and unpredictable artifacts or a measurable degradation of image quality can result. Many methods have been devised to scan objects larger than the largest FOV for which an instrument was designed.

X1.1.46 **filter, beam**—uniform layer of material, usually of higher atomic number than the specimen, placed between the radiation source and the film for the purpose of preferentially absorbing the softer radiations.

Discussion—Filters are used in CT scanners to reduce dose, scattered radiation, and beam-hardening effects.

X1.1.47 **filter, mathematical**—a function of spatial frequency giving weighting factors to use to modify each point of Fourier-transformed functions or numeric arrays. Application of such a filter to X-ray projection values is usually a step in the process of reconstructing CT images.

Discussion—Use of such a filter with an FFT is a common way of implementing a convolution. The filter is the Fourier transform of the corresponding convolution kernel.

X1.1.48 **focal spot**—the region at which the electrons are focussed in an X-ray machine or linear accelerator.

Discussion—The size of the resulting beam spot as seen from the object region is an important determinant of the aperture function, especially in the region near the radiation source. Since the spot does not generally have a sharp edge, quantitative values for spot size will reflect the method used to define it, since the average radius of, for example, the minimum region from which 99 % of the emission comes will be much larger than, say, the standard deviation of the intensity distribution.

X1.1.49 **gantry**—the mechanical apparatus in a tomographic scanner which controls the relative movement of the object to be examined and the source and detector mechanisms.

X1.1.50 **ionization detector**—a radiation detector in which the signal is produced by the collection of free electrons or ions directly produced by the radiation beam.

Discussion —Examples include xenon gas detectors and semiconductors such as mercuric iodide.

X1.1.51 **iterative reconstruction techniques**—successive-approximation methods using X-ray opacity measurements for computing an object description (typically a map of some density parameter), based on sequential adjustments of the description to make it consistent with the measurements.

Discussion—Algebraic reconstruction techniques (ART) are of this type. Contrasted with analytical reconstruction techniques.

X1.1.52 **kernel**—the set of numerical weights used in the convolution stage of the image-reconstruction process.

Discussion—The kernel and the associated frequency-space filter are Fourier transforms of each other.

X1.1.53 **keV**—kilo-electron-volts, a measure of energy.

Discussion—The photons used in industrial CT range in energy from a few keV to several thousand keV.

X1.1.54 **kV, kVp**—kilovolts, a measure of electrical potential.

Discussion—CT beams are often formed by accelerating electrons onto a metal target over voltages ranging from a few tens of kV up to several thousand kV. In each such case, the bremsstrahlung (braking radiation) photons formed by collisions in the target will range in energy from very small values up to a value in electron volts equal to the accelerating potential in volts.

X1.1.55 **laminogram, computed**—map of CT-density estimates of an object at positions on a two-dimensional surface, formed by backprojecting radiographic data (perhaps after mathematical filtering) onto the surface.

Discussion—Typically some blurred off-surface features remain in a laminographic image. The advantage of the technique is the ability to produce localized three-dimensional CT-density estimates from substantially less data than would be required for full three-dimensional reconstructions. Similar in many respects to the analog process of focal-plane tomography.

X1.1.56 **limited-data reconstruction**—a tomogram formed from an "incomplete" data set in which the object is sampled substantially more in some areas or directions than in others.

Discussion—Many forms of data limitation have been dealt with by special methods, including these types of reconstructions: few-angle (large angular steps between views), limited-angle (views missing over some range of directions, as when scanning a wall), limited-field (some portion of some views missing, typically due to high opacity or to positioning constraints), and region-of-interest (views consist of measurements through only a portion of the cross-section).

X1.1.57 **line-spread function**—see *edge response function*.

X1.1.58 **linear attenuation coefficient**—a measure of the fractional decrease in radiation beam intensity per unit of distance traveled in the material (cm^{-1}).

Discussion—The value of this parameter at each point in an object being examined by penetrating radiation depends on the composition of both the material and of the radiation beam passing through that region, as well as the density of the material. Units for this coefficient are typically cm^{-1}. The linear attenuation coefficient is the mass attenuation coefficient multiplied by the mass density of the substance. The CT

density in each pixel of a tomogram is basically a linear-attenuation-coefficient value, although artifacts may cause local or global deviations. This coefficient is the sum of the coefficients for several physical attenuation processes (see scattering, photoelectric absorption, and pair production), each of which varies substantially with the photon energy and the elemental composition of the material. The integral of linear attenuation coefficient along a ray path gives the X-ray projection value for that ray, which is measured in the dimensionless natural units called attenuation lengths.

X1.1.59 **linear detector array**—an array of radiation-sensing elements arranged in a one-dimensional sequence, typically uniformly spaced along an arc or straight line.

X1.1.60 **magnification**—the increase in the distance between rays as they proceed from the object to the detectors.

Discussion—Equal to the source-detector distance (SDD) divided by the source-object distance (SOD). Large magnifications are made practicable by the use of microfocus X-ray tubes, which give a very compact aperture function close to the source.

X1.1.61 **mass attenuation coefficient**—a measure of the fractional decrease in radiation beam intensity per unit of surface density $cm^2 \cdot gm^{-1}$.

Discussion—The value of this parameter at each point in an object being examined by penetrating radiation depends on the composition of both the material and of the radiation beam passing through that region. This coefficient, which is typically expressed in units of cm^2/g, is independent of the density of the substance; that is why it is generally what is given in tables rather than the related linear attenuation coefficient, which is the mass attenuation coefficient multiplied by the mass density.

X1.1.62 **mean free path**—the average distance traveled by an X-ray photon before it is scattered or absorbed by the material through which it is passing.

Discussion—See linear attenuation coefficient for a discussion of the factors involved.

X1.1.63 **measurement interlacing**—a tomographic scanning pattern of object motion and data reordering in which a finely-spaced fan-beam view is formed by interlacing a set of more-coarsely-spaced fans with a common vertex.

X1.1.64 **measurement spacing, CT**—the angular and linear separation between samples in each view and between view angles.

Discussion—The measurement spacing is a basic limit on spatial resolution, since it determines the scale at which reconstruction artifacts become unavoidable. For a fixed number of measurements, artifacts are generally minimized when the number of views is about equal to the number of measurements in each view. The measurement spacing is usually matched with the width of the aperture function to give samples which partially overlap but are still mostly independent.

X1.1.65 **modulation**—the extent to which the imaged densities of adjacent features of a given size or spacing are resolved in an image, expressed as a percentage of the actual density contrast.

Discussion—Used in specifications of spatial resolution to state the allowed amount of blurring at the specified line spacing.

X1.1.66 **modulation transfer function (MTF)**—a function giving the relative frequency response of an imaging system.

Discussion—The MTF is the normalized amplitude of the Fourier transform of the point spread function.

X1.1.67 **monitor detector**—a detector used to measure variations in the intensity of the source of penetrating radiation or some other system parameter.

Discussion—Also called reference detector.

X1.1.68 **monochromatic**—another term for monoenergetic, when applied to beams of X-rays.

X1.1.69 **monoenergetic**—comprised of photons all having the same energy.

Discussion—X-rays and gamma rays produced by the decay of a few radioisotopes, such as Americium-241 and Cesium-137, are essentially monoenergetic. Many theoretical concepts are defined in terms of monoenergetic beams. See also *multi-energetic*.

X1.1.70 **multienergetic**—comprised of photons with several different energies.

Discussion—Radiation produced by bremsstrahlung (sudden stopping of fast-moving electrons) in X-ray tubes or linear accelerators has a continuous multienergetic spectrum. See beam-hardening for a discussion of one of the consequences of making opacity measurements with a multienergetic beam.

X1.1.71 **noise**—the variation in a measurement (or in an estimate or image derived from measurements) when it is repeated under nominally identical conditions.

Discussion—Noise is distinguished from consistent biasing effects, which are referred to as artifacts in CT images. Averaging n independent measurements of the same object generally reduces the noise by a factor of the square root of n, as the random effects partially cancel each other. The noise in measurements of penetrating radiation has (in addition to a usually-small instrumental component) a photon statistics component determined by the measurement time, object opacity, radiation beam intensity, and detector aperture. In radiograms, this noise is almost uncorrelated, and its average value is inversely proportional to the square root of area for features which cover several pixels. Since the originally-independent measurements for a tomogram are mixed in the convolution and backprojection processes, the dependence of noise on feature size in a tomographic image is more complex.

X1.1.72 **non-linearity correction**—a function by which a measured signal is transformed so that the result has a linear relationship to the property being measured.

Discussion—The response of a tomographic detector to the radiation incident on it will not necessarily be linear. If the response is monotonic, however, it (or the X-ray projection values derived from it) can be transformed to linear by a function or table computed from an appropriate set of calibration measurements.

X1.1.73 **offset measurement**—see *dark measurement.*

X1.1.74 **opacity**—see *X-ray opacity*.

X1.1.75 **pair production**—the process whereby a gamma photon with energy greater than 1.02 MeV is converted directly into matter in the form of an electron-positron pair. Subsequent annihilation of the positron results in the production of two 0.511 MeV gamma photons.

Discussion—The minimum photon energy required for electron-positron pair production is 1.022 MeV (the rest mass of the two particles); any excess over this threshold goes into the kinetic energy of the particles. After the positron is stopped by interactions in the medium, it combines with an electron to form two 511 keV photons of annihilation radiation. The likelihood of pair production, which is directly proportional to the square of atomic number, increases with increasing energy, unlike the likelihood of scattering or absorption. This results in minimums in the opacity of matter to photons at energies from 300 MeV (hydrogen) to 9 MeV (iron) to 3.5 MeV (lead).

X1.1.76 **parallel beam**—a mode of arrangement of tomographic opacity measurements into sets of measurements made along parallel paths.

Discussion—Some scan geometries such as translate-rotate naturally produce a uniformly-spaced parallel-beam ray set for each detector; other scanning patterns can be used to produce parallel-beam views by reordering and/or interpolation. Contrasted to fan beam views.

X1.1.77 **partial-volume artifact**—an erroneous feature in a tomogram or radiogram due to inconsistent data caused by variation in the X-ray opacity on scales smaller than the width of the rays.

Discussion—Such high-frequency variation will usually result in an underestimate of the actual projected density, causing characteristic artifacts such as low-density lines aligned with straight edges in the object.

X1.1.78 **partial-volume effect**—the deviation of measured X-ray projection values from proportionality to average projected mass along a ray path, when projected mass changes rapidly within the width of the ray.

Discussion—This effect is most pronounced for rays along flat edges. See partial-volume artifact.

X1.1.79 **pencil beam**—beam of penetrating radiation collimated so that its dimensions in directions perpendicular to the beam axis are small compared to the source-object distance.

Discussion—Usually used with a single detector, as in "first-generation" CT scans.

X1.1.80 **phantom**—test object containing features of known size, spacing, and contrast, which can be scanned to determine spatial or density resolution.

Discussion—A variety of such standardized test objects are used with CT scanners for alignment of the systems, for calibration of image geometry and density mappings, and/or for determining the spatial and density resolution which can be achieved under specific scanning conditions. In some cases, small phantoms are included in production scans as image quality indicators.

X1.1.81 **photoelectric absorption**—a mode of interaction between photons and matter in which a photon is absorbed by an atom, which then emits an electron whose kinetic energy is the photon energy less the electron's binding energy.

Discussion—The likelihood of photoelectric absorption increases abruptly between energies just below and above the binding energies of electron shells, as more electrons become available for emission. Other than at these absorption edges, the photoelectric effect becomes less likely as the photon energy increases, decreasing as roughly the cube of the energy. Photoelectric absorption is strongly dependent on atomic number, with interactions with higher-atomic-number elements more likely by about the fourth power of the ratio of atomic numbers (on a per-atom basis; about the third power on a per-gram basis). For the photon energies used in industrial CT, photoelectric absorption is usually significant, and sometimes predominant, in both the process of attenuation in the object and the process of measurement of beam intensity in the detector. The primary competing process is Compton scattering, with elastic scattering and pair production also significant in some cases.

X1.1.82 **photon statistics**—the variation in intensity of a beam of photons (and thus in measurements derived from it) due to the randomness of emission of individual photons.

Discussion—This phenomenon sets a minimum level for the noise in the measurements, especially in cases where the total number of photons detected is small. The mathematical theory of Poisson statistics is relevant to this case; it predicts that such sampling variation will increase the noise in X-ray opacity estimates by a term whose variance is the reciprocal of the number of photons.

X1.1.83 **pixel (tomographic)**—one of a group of discrete positions composing a tomogram or related image.

Discussion—In general usage, pixels are the points on an image-display surface at which various colors and/or intensities may be shown. In computed tomography, the term is also often used to refer to the CT-density estimate computed for the corresponding physical position in the object being inspected. Because of interpolation or compression, the display pixels and the CT pixels in CT images may not represent areas of equal size. Pixels are usually arranged in rectangular arrays. The spatial resolution of a CT system is generally not determined by CT-pixel spacing, but rather by measurement spacing or by the aperture function. (If pixel size is so large as to limit resolution, the measured data can be used again to compute a tomogram of a subregion with pixels small enough that their size is not limiting.) The three-dimensional entity corresponding to the pixel is the voxel, or volume element.

X1.1.84 **point-spread function (PSF)**—the image of a small isolated point under an image-formation process, normalized to the total integrated density of the point.

Discussion—See spatial resolution, edge-response function, and modulation transfer function.

X1.1.85 **polychromatic**—another term for multienergetic, when applied to beams of X-rays.

X1.1.86 **projection**—the integral of a density function, typically along a straight line or a set of lines.

Discussion—The X-ray opacity measurements used in CT are projections of the linear attenuation coefficients along the ray paths. These are called X-ray projection values. A radiogram of an object is a two-dimensional projection.

X1.1.87 **radiation intensity**—the quantity of radiation per second passing through an area normal to the beam path.

X1.1.88 **radiation source**—the apparatus from which the penetrating radiation used in CT scans is emitted.

Discussion—Examples of industrial CT radiation sources are X-ray tubes, linear accelerators, radioisotopes, and synchotron radiation. The size of the radiation-emitting region, or beam spot, is an important determinant of the aperture function, and thus of the spatial resolution.

X1.1.89 **radiogram**—a two-dimensional projection of X-ray opacity recorded as a digitized array of computed values.

Discussion—Analogous to radiographs recorded on X-ray film. Such images, when produced by CT scanners, are also called by such names as preview scans or scout scans because of their use in selection of the desired slice plane. See digital radiography.

X1.1.90 **radioisotope**—an unstable isotype (type of atom), in which the nucleus will eventually change spontaneously, with the emission of particles and/or gamma rays.

Discussion —Several radioisotopes manufactured in nuclear reactors have been used as photon radiation sources for CT scanners, including isotopes of cobalt (^{60} Co), cesium (^{137} Cs), iridium (^{142} Ir), and americium (^{241} Am).

X1.1.91 **Radon transform**—a transform of a density function in two or more dimensions into its projections along straight lines.

Discussion—The Radon transform approximates the process of X-ray opacity measurement, and the basic image-reconstruction problem of computed tomography is finding an inverse to the projection transform. This problem was first solved by Radon in 1917.

X1.1.92 **ray**—the path taken by the penetrating radiation used in a particular X-ray opacity measurement.

Discussion—The aperture function gives the extent and intensity distribution of rays.

X1.1.93 **ray spacing**—the distance (linear or angular) between adjacent rays in a tomographic view.

Discussion—This distance is usually the most important determinant of spatial resolution. See measurement spacing.

X1.1.94 **rebinning**—production of a tomographic data set of a desired pattern (usually uniformly-spaced parallel-ray views) by redistribution or interpolation of the data set actually measured.

X1.1.95 **reconstruction**—the process of computing a description of an object from X-ray opacity measurements through it.

Discussion—Normal CT practice is to use CT-density values in a rectangular array of pixels or voxels to describe the object; such an array is called a tomogram. The standard method for computing tomograms groups opacity measurements into views which are convolved using Fourier transforms to apply a mathematical filter proportional to frequency. To each pixel in the tomogram is added a backprojected value from each convolved view, chosen based on which ray went through that pixel from that view. Other reconstruction techniques, notably successive-approximation methods, have also been developed but are not now in general use.

X1.1.96 **reference detector**—a detector used to measure variation in the source of penetrating radiation or some other system parameter.

Discussion—Also called monitor detector.

X1.1.97 **reformatting**—use of three-dimensional CT-density information to produce tomograms for surfaces other than the slice planes in which the X-ray opacities are measured.

Discussion —Most common is the production of two sets of planes orthogonal to the slice planes and to each other, but tomograms can also be interpolated in this way onto curved or discontinuous surfaces.

X1.1.98 **region-of-interest scan**—a tomographic scan in which only a limited portion of the object cross-section is included in all views.

Discussion—The amount and pattern of the artifacts due to the missing data depend strongly on the object shape, but are often acceptable within the boundaries of the fully-scanned region.

X1.1.99 **resolution**—the ability to distinguish features in an image.

Discussion—See spatial resolution, density resolution, and contrast-detail diagram.

X1.1.100 **scan, (CT or DR)**—set of measurements from which a tomogram or radiogram is to be computed, or the process of acquiring such measurements.

X1.1.101 **scan geometry**—the pattern and sequence of opacity measurement for a tomographic scan.

Discussion—Scan geometry is often specified by reference to the sequence of "generations" (first, second, third, fourth) of medical CT scanners. Second generation (translate-rotate) and third generation (rotate-rotate) geometries are most used in industrial CT. Another important scanning approach is cone beam geometry, in which an area detector is used.

X1.1.102 **scatter**—the redirection of radiation-beam photons due to interactions with matter in their path.

Discussion—Photons of the penetrating radiation used in tomography can interact with the electrons (or, at low energies, the nuclei) in a material in a manner which changes the direction of the photon. This scattering process has several implications for tomographic measurements: (1) the photon will generally not interact in the detector toward which it was originally travelling (causing attenuation of the primary beam), (2) the photon will usually transfer some of its energy to an electron in the material (causing dose in the object or signal in the detector), and (3) such a scattered photon may interact some detector not on its original path (introducing error into the associated opacity measurement). The contribution of scattered photons to measurements may be greatly reduced in some cases by collimation of the detector array or separation of the detector from the object; it is sometimes compensated for by subtracting an estimate of its value from the measurements. See Compton scattering and elastic scattering.

X1.1.103 **scintillation detector**—a device which converts incident radiation into visible light that is subsequently measured after conversion to an electrical signal.

X1.1.104 **SDD (source-to-detector distance)**—distance from radiation source to detector element.

X1.1.105 **second-generation scan**—a sequence of tomographic data acquisition in which the object being examined is translated across a fan beam several times, with the object rotated by the detector-array fan angle after each pass.

Discussion—The primary advantages of such translate-rotate scans are the natural production of parallel-beam views (which are easier to process), the use of a single detector for all measurements in a view (which eliminates some types of artifacts), and more flexibility in the size of object which can be scanned. The primary disadvantage compared to third-generation scans is the extra motion time required.

X1.1.106 **sharpening**—a transformation of a view or image in which the differences between points located near to each other are increased relative to differences between more separated points.

Discussion—An important class of such transforms are filters which increase the high-frequency content of images. Sharpening typically increases noise but may also increase spatial resolution, up to the limit imposed by measurement spacing. The convolution step in tomographic image formation includes a particular type of sharpening. See also smoothing, which is the opposite process.

X1.1.107 **sinogram**—the set of X-ray opacity values obtained during a tomographic scan, typically ordered as a two-dimensional array (position within view vs. view angle).

X1.1.108 **slice, CT**—a tomogram or the object cross-section corresponding to it.

Discussion—The slice plane is the plane, determined by the focal spot and the linear array of detectors, around which each measurement of a planar tomographic scan is centered. Each such scan also has a slice thickness, which is the distance normal to the slice plane over which changes in object opacity will significantly influence the measurements; typically an average value based on the aperture function is used to characterize this parameter. When three-dimensional CT-density maps have been reconstructed, a slice may be formed on an arbitrary plane or other surface, not just on slice planes.

X1.1.109 **slice plane**—the plane, determined by the focal spot and the linear array of detectors, around which each measurement of a planar tomographic scan is centered.

Discussion —Not applicable to cone-beam scan geometries. Using three-dimensional techniques such as reformatting, images may be formed on planes other than the original slice plane.

X1.1.110 **slice thickness**—the average distance normal to a fan of radiation over which changes in object opacity will significantly influence the signal generated in detectors at which the fan is directed.

Discussion—Typically an average value based on the aperture function in the region of the object is used to characterize this parameter. See beam width.

X1.1.111 **smoothing**—a transform of a tomographic view or image in which the difference between nearby points is reduced.

Discussion—Smoothing typically reduces noise but also decreases spatial resolution. Smoothing may be linear (such as local averaging) or nonlinear (such as median filtering). For tomograms, linear smoothing (or sharpening, the inverse process) can be applied without additional computation by suitable modification of the convolution filter used in image formation.

X1.1.112 **SOD (source-to-object distance)**—distance from radiation-source beam spot to the center of rotation of the object.

X1.1.113 **source spot**—the small region from which penetrating radiation is emitted from radiation sources used in radiographic imaging.

Discussion—The size of a source spot as seen from the region of the object is an important limit on the sharpness of an image formed with its radiation, with smaller spots giving sharper images. However, smaller spots also give less intense (and thus noisier) radiation beams. For X-ray machines, which produce source spots of from 2 mm (0.079 in.) down to 0.005 mm (0.0002 in.), the limit on maximum intensity is due to the melting point of the tungsten anode. For a radioisotope, the intensity limit is due to a combination of its half-life, concentration, density, gamma-ray multiplicity, self-attenuation, and energy spectrum. The brightest radioisotopes used in industrial imaging, ^{192}Ir and ^{60}Co, are much less intense than X-ray machines per unit of source-spot area.

X1.1.114 **spatial resolution, CT**—the extent to which a tomogram or radiogram can be used to detect details of the shape of image features whose contrast is substantially greater than the image noise.

Discussion—CT spatial resolution is best characterized by the point-spread or line-spread functions of the image, or by the equivalent modulation transfer function (MTF) in frequency space. The spatial resolution is generally limited by the measurement spacing (which in turn is often influenced by the aperture function), not by the spacing of the pixel grid. For assessing the information in images in which noise is significant, a contrast-detail diagram should be used.

X1.1.115 **third-generation scan**—a sequence of tomographic data acquisition in which the object being examined is rotated relative to the radiation source and detectors.

Discussion —This "pure rotation" methodology has the advantages of speed and efficient use of the detector array, but requires careful calibration to avoid circular artifacts. The most common mode of scanning in medical CT; also common in industrial CT.

X1.1.116 **tomogram**—map of CT-density estimates of an object at positions on a two-dimensional surface, typically a square grid on a cross-sectional plane.

X1.1.117 **translation**—motion of the object being examined relative to the tomographic measurement apparatus, generally in a straight line.

Discussion—Contrasted to rotation of the object or apparatus. Linear translation can be used to produce a parallel-ray view with each detector (see second-generation scan). On fan beam systems, translation normal to the slice plane is used to produce digital radiograms.

X1.1.118 **view, CT**—a set of X-ray opacity projection values (derived from measurements or by simulation) grouped together for processing purposes, especially for the convolution and backprojection steps of computing a tomogram.

Discussion—The rays forming a view will usually be parallel (parallel-beam views) or have a common vertex at the radiation source (fan-beam views). The pattern of rays in views need not be the same as that of the measurements, since they can be sorted or interpolated.

X1.1.119 **voxel**—volume element; one of a group of positions or small volumes at which some density parameter of an object is estimated in a three-dimensional tomographic reconstruction.

Discussion—See pixel.

X1.1.120 **window (density)**—the range of pixel values in a tomogram or other image which are presented to the viewer as varying intensities on a graphics display monitor.

Discussion —Typically, values above or below the current density window are all shown as the same color, such as black or white. The width of the window can be a small fraction of the full range of the image density values; changing the position and size of the density window within the full range permits display of all features, even in images whose full dynamic range exceeds that of human visual inspection. The mapping of image-density values to colors or gray-scale intensities is usually linear, but can be changed to other modes, such as logarithmic compression or histogram equalization.

X1.1.121 **X-ray opacity**—the extent to which an object attenuates X-ray radiation passing through it.

Discussion—Because such attenuation is an exponential function of the amount of material penetrated, opacity is measured in attenuation lengths, which are the normal logarithm of the ratio of the amount of radiation entering an object to the amount which passes through it without interaction. The opacity along many straight-line ray paths through an object is the information from which tomograms are computed. While the opacity of a material to mono-energetic radiation is independent of detector efficiency and directly proportional to material thickness, beam-hardening corrections may be required to correctly infer thickness from opacity measurements with multienergetic X-ray beams.

REFERENCES

(1) Evans, R. D., *The Atomic Nucleus*, McGraw-Hill Book Company, New York, NY, 1955.

(2) Robb, R. A., et al, "High-Speed Three-Dimensional X-Ray Computed Tomography: The Dynamic Spatial Reconstructor," *Proceedings IEEE*, Vol 71, 1983, pp. 308–319.

(3) Glenn, W. V., et al, "Image Manipulation and Pattern Recognition," *Radiology of the Skull and Brain*, Vol 5: "Technical Aspects of Computed Tomography," C.V. Mosby Company, 1981, pp. 4326–4354.

(4) Radon, J., "Über die Bestimmung von Funktionen durch Ihre Intergralwerte Längs Gewisser Mannigfaltigkeiten," Saechsische Akademie der Wissenschaftten, Leipzig, *Berichte über die Verhandlungen*, Vol 69, 1917, pp. 262–277.

(5) Bracewell, R. N., "Strip Integration in Radio Astronomy," *Australian Journal of Physics*., Vol 9, 1956, pp. 198–217.

(6) Oldendorf, W. H., "Isolated Flying-Spot Detection of Radiodensity Discontinuities; Displaying the Internal Structural Pattern of a Complex Object," *IRE Transactions on Bio-Medical Electronics*, Vol BME-8, 1961, pp. 68–72.

(7) Kuhl, D. E., and Edwards, R. Q., "Image Separation Radioisotope Scanning," *Radiology*, Vol 80, 1963, pp. 653–662.

(8) Cormack, A. M., "Representation of a Function by Its Line Integrals, with Some Radiological Applications," *Journal of Applied Physics*, Vol 34, 1963, pp. 2722–2727.

(9) De Rosier, D. J., and Klug, A., "Reconstruction of ThreeDimensional Structures from Electron Micrographs," *Nature*, Vol 217, 1968, pp. 130–134.

(10) Smith, P. R., et al," Studies of the Structure of the T4 Bacteriophage Tail Sheath. I. The Recovery of Three-Dimensional Information from the Extended Sheath," *Journal of Molecular Biology*, Vol 106, 1976, pp. 243–275.

(11) Moore, W. E., and Garmire, G. P., "The X-Ray Structure of the Vela Supernova Remnant," *The Astrophysics Journal*, Vol 199, 1975, pp. 680–690.

(12) Brooks, R. A., and Di Chiro, G., "Principles of Computer Assisted Tomography (CAT) in Radiographic and Radioisotopic Imaging," *Physics in Medicine and Biology*, Vol 21, 1976, pp. 689–732.

(13) Newton, T. H., and Potts, D. G., Eds., *Radiology of the Skull and Brain*, Vol 5: "Technical Aspects of Computed Tomography," C.V. Mosby Company, 1981.

(14) Raviv, J., et al, Eds., *Computer Aided Tomography and Ultrasonics in Medicine*, North-Holland Publishers, Amsterdam, The Netherlands, 1979.

(15) Greenleaf, J. F., "Computerized Tomography with Ultrasound," *Proceedings IEEE*, Vol 71, 1983, pp. 330–337.

(16) Lauterbur, P. C., "Medical Imaging by Nuclear Magnetic Resonance Zeugmatography," *Transactions on Nuclear Science*, IEEE, Vol NS-26, 1979, pp. 2808–2811.

(17) Altschuler, M. D., and Perry, R. M., "On Determining the Electron Distributions of the Solar Corona from K-Coronameter Data," *Solar Physics*, Vol 23, 1972, pp. 410–428.

(18) Hanson, K. M., "Proton Computed Tomography," *Computer Aided Tomography and Ultrasonics in Medicine*, North-Holland Publishers, Amsterdam, The Netherlands, 1979, pp. 97–106.

(19) Budinger, T. F., et al, "Emission Computed Tomography," *Image Reconstruction from Projections: Implementation and Applications*, Springer-Verlag, Berlin and New York, 1979.

(20) Knoll, G. F., "Single-Photon Emission Computed Tomography," *Proceedings IEEE*, Vol 71, 1983, pp. 320–329.

(21) Ter-Pogossian, M. M., "Positron Emission Tomography," *Scientific American*, Vol 243, 1980, pp. 171–181.

(22) *Handbook of Chemistry and Physics*, 45th ed., Chemical Rubber Company, 1964–1965, p. F-47.

(23) Logan, B. F., "The Uncertainty Principle in Reconstructing Functions from Projections," *Duke Mathematical Journal*, Vol 42, 1975, pp. 661–706.

(24) Huesman, R. H., "The Effects of a Finite Number of Projection Angles and Finite Lateral Sampling of Projections on the Propagation of Statistical Errors in Transverse Section Reconstruction," *Physics Med. Biol*., Vol 22, 1977, pp. 511–521.

(25) Snyder, D. L., and Cox, J. R.," An Overview of Reconstructive Tomography and Limitations Imposed by a Finite Number of Projections," *Reconstruction Tomography in Diagnostic Radiology and Nuclear Medicine*, University Park Press, Baltimore, MD, 1977, p. 28.

(26) Gore, J. C., and Tofts, P. S., "Statistical Limitations in Computed

Tomography," *Physics in Medicine and Biology*, Vol 23, 1978, pp. 1176–1182.
(27) Seitz, P., et al, "The Influence of Photon Counting Statistics on Picture Noise and Reproducibility in Quantitative Tomography," *Transcripts Nuclear Science*, IEEE, Vol NS-32, 1985, pp. 1162–1168.
(28) Joseph, P. M., "Artifacts in Computed Tomography," *Radiology of the Skull and Brain*, Vol 5: "Technical Aspects of Computed Tomography," C.V. Mosby Company, 1981, pp. 3956–3992.
(29) Dennis, M. J., "Technical Notes on the Use of the General Electric CT 9800," *General Electric Medical Systems*, General Electric Company, 1984.
(30) Haque, P., and Stanley, J. H., "Basic Principles of Computed Tomography Detectors," *Radiology of the Skull and Brain*, Vol 5: "Technical Aspects of Computed Tomography," C.V. Mosby Company, 1981, pp. 4096–4103.
(31) Peschmann, K., "An Upper Limit on the Nonlinearity of Scintillator-Photodiode Detectors," Report by Radiological Imaging Laboratory to ARACOR on Subcontract W-0262 with Bureau of Alcohol, Tobacco and Firearms, 1981.
(32) Hounsefield, G. N., "Some Practical Problems in Computed Tomography Scanning," *Reconstruction Tomography in Diagnostic Radiology and Nuclear Medicine*, 1977, pp. 217–223.
(33) Hanson, K. M., "Detectability in Computed Tomographic Images," *Medical Physics*, Vol 6, 1979, pp. 441–451.
(34) Brooks, R. A., and Di Chiro, G., "Beam Hardening in X-Ray Reconstructive Tomography," *Physics in Medicine and Biology*, Vol 21, 1976, pp. 390–398.
(35) Herman, G. T., "Correction for Beam Hardening in Computed Tomography," *Physics in Medicine and Biology*, Vol 24, 1979 , pp. 81–106.
(36) Alvarez, R. E., and Macovski, A., "Energy-Selective Reconstructions in X-Ray Computerized Tomography," *Physics in Medicine and Biology*, Vol 21, 1976, pp. 733–744.
(37) Bracewell, R. N., "Correction for Collimator Width (Restoration) in Reconstructive X-Ray Tomography," *Journal of Computer Assisted Tomography*, Vol 1 , 1977, pp. 6–15.
(38) Joseph, P. M., and Spital, R. D., "The Exponential Edge-Gradient Effect in X-Ray Computed Tomography," *Physics in Medicine and Biology*, Vol 26, 1981, pp. 473–487.
(39) Yester, M. W., and Barnes, G. T., "Geometrical Limitations of Computed Tomography (CT) Scanner Resolution," *ProceedingsApplied Optical Instrumentation in Medicine*, SPIE, Vol VI 127, 1977, pp. 296–303.
(40) Stonestrom, J. P., and Macovski, A., "Scatter Considerations in Fan Beam Computerized Tomographic Systems," *Transactions on Nuclear Science IEEE*, Vol NS-23, 1976, pp. 1453–1458.
(41) Cormack, A. M., "Representation of a Function by Its Line Integral, with Some Radiological Applications, II," *Journal of Applied Physics*, Vol 35, 1964, pp. 2908–2913.
(42) Censor, Y., "Finite Series-Expansion Reconstruction Methods," *Proceedings* IEEE, Vol 71, 1983, pp. 409–419.
(43) Hounsfield, G. N., "A Method and Apparatus for Examination of a Body by Radiation such as X or Gamma Radiation," *Patent Spec. 1283915*, The Patent Office, London, UK.
(44) Gordon, R., et al, "Algebraic Reconstruction Techniques (ART) for Three-Dimensional Electron Microscopy and X-Ray Photography," *Journal of Theoretical Biology*, Vol 29, 1970, pp. 471–481.
(45) Herman, G. T., et al, "ART: Mathematics and Applications," *Journal of Theoretical Biology*, Vol 42, 1973, pp. 1–32.
(46) Herman, G. T., and Lent, A., *A Family of Iterative Quadratic Optimization Algorithms for Pairs of Inequalities, with Application in Diagnostic Radiology*, Mathematical Programming Study 9, 1978, pp. 15–78.
(47) Baba, N., and Murata, K., "Maximum Entropy Image Reconstruction from Projections," Technical Report, Department of Applied Physics, Hokkai-do University, Sapporo 060, Japan.
(48) Minerbo, G., "MENT: A Maximum Entropy Algorithm for Reconstructing A Source from Projection Data," *Computer Graphics and Image Processing*, Vol 10, 1979, pp. 48–68.
(49) Tasto, M., and Schomerg, H., "Object Reconstruction from Projections and Some Nonlinear Extensions," *Pattern Recognition and Signal Processing*, Sijthoff and Noordhoft, Amsterdam, The Netherlands, 1978, pp. 485–503.
(50) Schomberg, H., "Nonlinear Image Reconstruction from Projection of Ultrasonic Travel Times and Electric Current Densities," *Mathematical Aspects of Computerized Tomography (Lecture Notes in Medical Informatics)*, Vol 8, Springer, Berlin, 1981, pp. 270–291.
(51) Barton, J. P., et al, "Computerized Tomography for Industrial Applications," Technical Report IRT 4617-011, IRT Corporation, San Diego, CA, Feb. 1979.
(52) Gullberg, G. T., *The Attenuated Radon Transform: Theory and Application in Medicine and Biology* , PhD Dissertation, Technical Report LBL-7486, Donner Lab., University of California, Berkeley, CA, March 1980.
(53) Natterer, F., "The Identification Problem in Emission Computed Tomography," *Mathematical Aspects of Computerized Tomography (Lecture Notes in Medical Informatics)*, Vol 8, 1981, pp. 45–56.
(54) Oppenheim, B. E., "Reconstruction Tomography from Incomplete Projections," *Reconstruction Tomography in Diagnostic Radiology and Nuclear Medicine*, 1977, pp. 155–183.
(55) Lewitt, R. M., and Bates, R. H. T., "Image Reconstruction from Projections, IV: Projection Completion Methods (Computational Examples)," *Optik*, Vol 50, 1978, pp. 269–278.
(56) Ritman, E. L., et al, "Quantitative Imaging of the Structure and Function of the Heart, Lungs, and Circulation," *Mayo Clinic Proceedings*, Vol 53, 1978, pp. 3–11.
(57) Schlindwein, M.," Iterative Three-Dimensional Reconstruction from Twin-Cone Beam Projections," *Transactions on Nuclear Science*, IEEE, Vol NS-25, 1978, pp. 1135–1143.
(58) Bracewell, R. N., and Riddle, A. C., "Inversion of Fan-Beam Scans in Radio Astronomy," *Astrophysics Journal*, Vol 150, 1967, pp. 427–434.
(59) Ramachandran, G. N., and Lakshminarayanan, A. V., "ThreeDimensional Reconstruction from Radiographs and Electron Micrographs: Application of Convolutions Instead of Fourier Transforms," *Proceedings of the National Academy of Sciences USA*, Vol 68, 1970, pp. 2236–2240.
(60) Herman, G. T., and Rowland, S. W., "Three Methods for Reconstructing Objects from X-rays: A Comparative Study," *Computer Graphics Image Processing*, Vol 2, 1973, pp. 151–178.
(61) Stark, H. H., et al, "Direct Fourier Reconstruction in Computer Tomography," IEEE Transactions on Acoustics, Speech, and Signal Processing ASSP-29, 1981, 237–245.
(62) Bates, R. H. T., and Peters, T. M., "Towards Improvements in Tomography," *New Zealand Journal of Science*, Vol 14, 1971, pp. 883–896.
(63) Lewitt, R. M., "Reconstruction Algorithms: Transform Methods," *Proceedings IEEE*, Vol 71, 1983, pp. 390–408.
(64) Low, K. H., and Natterer, F., "An Ultra-Fast Algorithm in Tomography," *Technical Report A81/03*, Fachbereich Angewandte Mathematik und Informatik, Universitat des Saarlandes, 6600 Saarbrucken, West Germany, 1981.
(65) Flannery, B. P., Roberge, W. G., and Deckman, H. W., "Computed Tomography by Direct Fourier Inversion: Fast Methods for X-ray Microtomography," Exxon Research and Engineering Company, Vol 237, 1987, pp. 1439–1444.
(66) Bracewell, R. N., "Image Reconstruction in Radio Astronomy," *Image Reconstruction from Projections: Implementation and Applications*, 1979, pp. 81–103.
(67) Hinshaw, W. S., and Lent, A. H., "An Introduction to NMR Imaging: From the Bloch Equation to the Imaging Equation," *Proceedings IEEE*, Vol 71, 1983, pp. 338–350.

(68) Greivenkamp, J. E., et al, "Incoherent Optical Processor for X-Ray Transaxial Tomography," *Applied Optics*, Vol 20, 1981, pp. 264–273.
(69) Sato, T., et al, "Tomographic Image Reconstruction from Limited Projections Using Coherent Optical Feedback," *Applied Optics*, Vol 20, 1981, pp. 3073–3076.
(70) Macovski, A., *Medical Imaging Systems*, Prentice-Hall, Inc., Englewood Cliffs, NJ, 1983.
(71) Glover, G. H., and Eisner, R. L., "Theoretical Resolution of CT Systems," *Journal of Computer Assisted Tomography*, Vol 3, No. 1, 1979, pp. 85–91.
(72) Yester, M. W., and Barnes, G. T., "Geometrical Limitations of Computed Tomography (CT) Scanner Resolution," *Proceedings Applications of Optical Instrumentation in Medicine*, SPIE, Vol VI 127, 1977, pp. 296–303.
(73) Ramachandran, G. N., and Lakshminarayanan, A. V., "ThreeDimensional Reconstruction from Radiographs and Electron Micrographs: Application of Convolutions Instead of Fourier Transforms," *Proceedings of the National Academy of Science*, USA, Vol 68, 1970, pp. 2236–2240.
(74) Shepp, L. A., and Logan, B. F., "Reconstructing Interior Head Tissue From X-Ray Transmissions," *IEEE Transactions on Nuclear Science*, Vol NS-21, 1974, pp. 228–236.
(75) Judy, P. F., "Line-Spread Function and Modulation-Transfer Function of a Computed Tomographic Scanner," *Medical Physics*, Vol 3, No. 4, 1976, pp. 233–236.
(76) Barrett, H. H., and Swindell, W., *Radiological Imaging*, Vol 2, Academic Press, New York, NY, 1981.
(77) Hanson, K. M., "Detectability in the Presence of Computed Tomographic Reconstruction Noise," *SPIE Optical Instrumentation in Medicine VI*, Vol 27, 1977, pp. 304–312.
(78) Hanson, K. M., "Detectability in Computed Tomographic Images," *Medical Physics*, Vol 6, No. 5, 1979, pp. 441–451.
(79) Sekihara, K., Kohno, H., and Yamamoto, S., "Theoretical Prediction of X-ray CT Image Quality Using Contrast Detail Diagrams," *IEEE Transactions on Nuclear Science*, Vol NS-29, 1982, pp. 2115–2121.
(80) Cohen, G., and Di Bianca, F., "The Use of Contrast-Detail-Dose Evaluation of Image Quality in a CT Scanner," *Journal of Computer Assisted Tomography*, Vol 3, No. 2, 1979, pp. 189–195.
(81) McMaster, W. H., Del Grande, N. K., Mallett, H. H., and Hubbell, J. H., *Compilation of X-ray Cross Sections*, University of California Radiation Laboratory, UCRL-50173-SEC 2-R-1.
(82) Hubbell, J. H., Gimm, H. A., and Overbo, I., "Pair, Triplet, and Total Atomic Cross-Sections (and Mass Attenuation Coefficients) for 1 MeV-100 GeV Photons in Elements A = 1 to 100," *Journal of Chemical Physics Reference Data*, Vol 9, No. 4, 1980, pp. 1023–1148.
(83) Dennis, M. J., "Industrial Computed Tomography," ASM Handbook Volume 17: Nondestructive Evaluation and Quality Control, ASM International, 1989, pp. 358–386.

SUMMARY OF CHANGES

Committee E07 has identified the location of selected changes to this standard since the last issue (E1441 - 00(2005)) that may impact the use of this standard. (July 1, 2011)

(1) Deleted metrological limits in 1.6. Technology changes have rendered these values obsolete
(2) Deleted timing reference in 1.10since it is was too limiting; and deleted sentence on limitation of volumetric CT.
(3) Changed 1.12 to state that this standard is an SI standard with hard conversions to inch-pound units.
(4) Deleted Ionization Detectors in 6.4.1since they are obsolete technology for CT.
(5) Added descriptions of several additional scan geometries in 6.5.1.5.
(6) Added sentence to 6.5.2 describing use of volumetric CT.
(7) Deleted obsolete information regarding computer systems in6.6.
(8) Deleted obsolete information on data storage media in 6.8.
(9) Add reference (**83**).